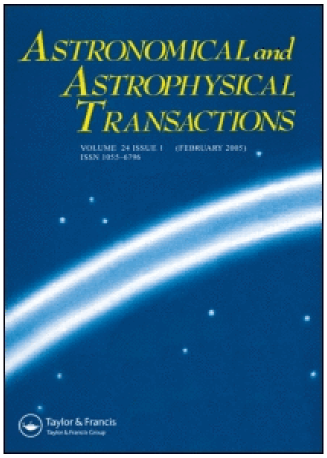

Astronomical & Astrophysical Transactions
The Journal of the Eurasian Astronomical Society
Publication details, including instructions for authors and subscription information:
http://www.informaworld.com/smpp/title~content=t713453505

Flat edge-on galaxies. Atlas and photometry

I. D. Karachentsev [a]; Ts. B. Georgiev [b]; S. S. Kajsin [a]; A. I. Kopylov [a]; V. P. Ryadchenko [a]; V. S. Shergin [a]
[a] Special Astrophysical Observatory of the USSR Academy of Sciences, Stavropol Territory, USSR
[b] Department of Astronomy and National Astronomical Observatory of the Bulgarian, Academy of Sciences, Sofia, Bulgaria

Online Publication Date: 01 October 1992
To cite this Article: Karachentsev, I. D., Georgiev, Ts. B., Kajsin, S. S., Kopylov, A. I., Ryadchenko, V. P. and Shergin, V. S. (1992) 'Flat edge-on galaxies. Atlas and photometry', Astronomical & Astrophysical Transactions, 2:4, 265 - 325
To link to this article: DOI: 10.1080/10556799208205344
URL: http://dx.doi.org/10.1080/10556799208205344

Astronomical and Astrophysical Transactions, 1992,
Vol. 2, pp. 265–325
Reprints available directly from the publisher.
Photocopying permitted by license only

FLAT EDGE-ON GALAXIES. ATLAS AND PHOTOMETRY

I. D. KARACHENTSEV,[1] TS. B. GEORGIEV,[2] S. S. KAJSIN,[1]
A. I. KOPYLOV,[1] V. P. RYADCHENKO,[1] and V. S. SHERGIN[1]

[1]*Special Astrophysical Observatory of the USSR Academy of Sciences, Stavropol Territory, 357147, USSR*
[2]*Department of Astronomy and National Astronomical Observatory of the Bulgarian Academy of Sciences, Sofia 1784, Bulgaria. Visiting Astronomer at the SAO, USSR AS*

(Received October 31, 1991; in final form January 17, 1992)

For a complete sample of 120 northern galaxies with angular diameters $10 \geqslant a \geqslant 2$ arc minutes and apparent aspect ratio $a/b \geqslant 7$, CCD observations were carried out in the R'-passband. We present the isophotal images of the galaxies, their luminosity profiles and some basic photometric parameters. The isophotal aspect ratio for most flat galaxies turns out to be smaller than that given in catalogues and does not exceed $(a/b)_{max} = 15$. We note a diversity of the galactic luminosity profiles and propose a classification based on the degree of deviation from the standard exponential law. About two-third of the flat galaxies have nonstandard profiles; however, this hardly can be attributed to strong internal absorption within edge-on galaxies.

KEY WORDS spiral galaxies, photometric profiles

1. INTRODUCTION

Late-type (Sc-Sd) spiral galaxies, which are visible edge-on, have an apparent aspect ratio $a/b > 7$. Hereafter they are referred to as "flat" galaxies. A photograph of their representative, NGC 100 = UGC 231, is presented in Figure 1. A simple geometric criterion, $a/b > 7$, allows to select nearby bulgeless objects and to produce thereby morphologically homogeneous sample among rather remote galaxies. An important property of the flat galaxies is existence of a tight correlation between their linear diameters and HI-linewidths (Karachentsev, 1989), which opens possibilities for studies of large-scale non-Hubble streamings in the Universe.

An expected internal absorption of light in flat galaxies is rather high. This is one of the reasons why the structure and kinematics of flat edge-on galaxis as yet have not been studied systematically. Just recently optical rotation curves were obtained for 50 flat galaxies (Karachentsev and Zhou Xu, 1991; Karachenstsev, 1991a). Detailed photometric data is presently available only for a dozen of galaxies with $a/b > 7$ (Watanabe, 1983; Fouque and Paturel, 1983; van der Kruit and Searle, 1981, 1982; Skrutskie *et al.*, 1985; Meisels, 1985).

Scantiness of the available data on detailed photometry of Sc edge-on galaxies prompted us to undertake a special observational program, with a result that the total number of studied objects is increased now by an order of magnitude.

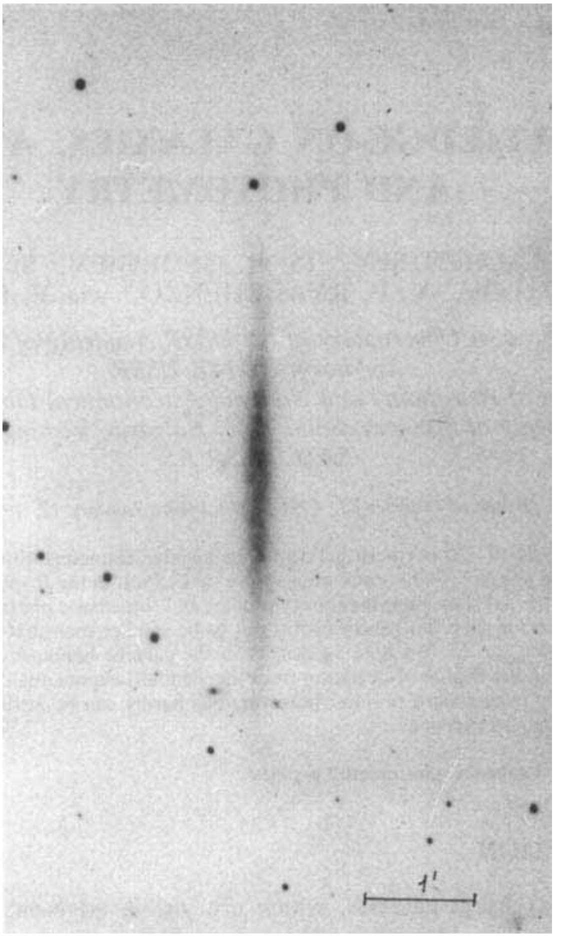

Figure 1 A print of the flat galaxy UGC 231 = NGC 100. The photograph was obtained by N. Tikhonov in the RC focus of 1-m telescope at Sanglok mountain. The seeing was 1 arc second, the exposure time was 4 hours.

2. OBSERVATIONS

Our observational program embraces northern galaxies (DEC > 0°) of the angular diameter $a \geqslant 2$ arc. min. and the apparent axial ratio $a/b > 7$, as given in the UGC-catalogue by Nilson (1973). Angular diameters of galaxies are inferred from measurements on blue prints of the Palomar Sky Survey. Altogether, with the UGCA-supplement (Nilson, 1974), there are 126 objects satisfying the conditions mentioned.

Observations of the chosen flat galaxies were performed with the CCD-camera attached to the focal reducer in the prime focus of the 6-meter telescope during several sessions between September 1989 and December 1990. The CCD-detector of the format 512×512 and pixel size $18 \times 24\,\mu$m provides the view field of

Table 1

UGC	V_h	W	T	a/b	a_{23}	a_{24}	m_{23}	m_{24}	SB_0	SB_0^d	PI
1	2	3	4	5	6	7	8	9	10	11	12
231	841	210	c	7.0	84	122	13.14	12.85	20.4	20.0	0
290	758	100	Ir:	5.6	17	43	17.40	16.25	21.9	22.5	-1
418	4438	382	b	5.5	46	59	13.95	13.77	19.4	20.9	-2:
485	5238	359	c	8.3	60	68	13.98	13.74	20.5	20.6	2
507	5277	455	c	7.0	59	68	13.41	13.23	19.9	20.3	2
542	4508	368	-	4.0	45	62	13.34	13.18	19.0	20.4	-1
711	1978	202	c	9.0	71	89	14.44	14.02	21.1	21.1	0
1400	5536	-	b	4.6	64	86	12.02	11.94	18.0:	20.7	-3
1650	4585	235	c	4.5	20	27	15.83	15.53	20.8	20.5	0
1839	1535	142	dm	5.9	41	56	15.13	14.55	21.3	21.1	0
1867	5195	281	c	6.7	46	54	14.73	14.44	20.4	20.8	1:
1970	1915	228	c	5.8	51	60	14.14	13.88	20.5	20.6	1
2092	6120	452	c	9.2	63	76	14.37	14.03	20.1	21.0	-1
2101	5835	500	b	5.1	50	63	13.70	13.55	19.4	20.1	-1
2370	2162	194	-	7.6	44	56	15.20	14.85	20.8	21.2	1
2411	2546	312	-	12.0	75	101	15.04	14.38	21.4	21.5	0
3326	4085	528	c	11.2	89	122	13.49	13.22	19.8	20.4	0
3365	5150	537	a:	4.4	50	59	13.24	13.10	19.2	20.2	-1
3425	4057	419	b	5.1	59	71	13.42	13.20	19.6	20.6	-1
3474	3633	360	c	7.6	61	72	13.72	13.51	20.2	20.4	2
3489	5455	475	bc	6.0	37	57	14.80	14.45	20.3	20.5	0
3539	3305	312	bc	5.5	40	56	14.46	14.17	20.0	20.3	0
3597	-	-	-	4.2	39	56	13.82	13.65	18.9	19.9	-1
3697	3136	262	-	10.6	96	110	13.45	13.14	20.2	20.2	1
3782	2269	336	c	7.6	101	110	12.87	12.70	19.6	20.3	-1
3879	4797	250	c	4.2	33	45	15.13	14.70	20.7	21.2	0
3959	3109	425	b	5.6	78	101	12.54	12.40	18.6	19.8	-1
4043	3401	419	c	6.2	54	61	13.76	13.58	20.2	20.2	2
4148	736	135	dm	5.3	21	41	16.70	15.77	22.0	22.0	0
4257	4164	243	c	6.4	39	52	15.12	14.77	21.0	21.0	0
4259	3832	397	b	4.4	48	67	13.40	13.17	18.7	20.7	-2
4277	5459	575	c	6.8	74	98	13.54	13.23	20.0	20.9	-1
4278	563	180	c	9.3	118	132	13.00	12.62	20.6	20.6	2
4550	2068	264	b	4.4	45	66	14.20	13.87	20.3	20.9	-1
4704	596	129	dm	6.7	47	94	15.33	14.38	21.8	21.8	0
4719	5116	542	c	6.5	62	73	13.35	13.19	19.2	20.0	-1:
4961	1578	324	c	6.0	72	105	13.06	12.81	20.2	19.3	1:

Table 1 (*Continued*)

UGC	V_h	W	T	a/b	a_{23}	a_{24}	m_{23}	m_{24}	SB_0	SB_0^d	PI
1	2	3	4	5	6	7	8	9	10	11	12
5173	6237	491	b	7.1	60	73	13.96	13.69	20.1	21.3	-1:
5203	1551	190	c	7.7	55	70	14.62	14.27	20.9	20.9	1
5210	4441	304	c	5.0	40	59	14.96	14.44	21.0	21.0	0
5341	7568	607	c	9.3	68	82	14.24	13.92	20.2	20.9	-1:
5389	6980	352	c	7.7	46	56	14.89	14.58	20.7	20.8	1
5452	1342	200	bc	5.2	52	71	13.92	13.64	19.8	20.6	-1
5459	1110	264	c	5.7	111	135	12.25	12.15	-	-	-
5495	8249	569	c	5.4	55	73	13.91	13.64	19.5	20.8	-1
5537	3756	288	c	7.7	48	62	14.83	14.47	20.8	20.9	0
5662	1324	173	b	8.1	48	80	14.67	14.24	20.6	21.4	-1
5687	3563	258	c	6.3	46	58	14.67	14.33	20.6	21.0	1
5741	1391	325	c	8.5	76	88	12.70	12.55	19.7	19.7	3
6080	2180	190	c	5.8	38	51	15.57	14.99	21.5	21.5	1
6116	1134	304	c	8.5	103	118	12.52	12.36	19.4	19.9	1
6483	3891	324	c	4.7	39	51	14.00	13.80	19.8	19.8	0
6497	6324	384	dm	8.4	46	54	15.20	14.80	21.1	21.2	2
6594	1040	171	c	5.6	52	65	14.52	14.12	20.8	21.2	1
6667	978	176	c	7.2	74	97	13.90	13.50	20.9	21.0	1
6686	6546	402	b	6.6	55	72	14.10	13.83	19.4	21.1	-2
6774	2417	228	c:	4.1	29	45	14.25	14.07	19.7	21.1	-1
6802	1256	139	c	4.9	43	58	14.58	14.21	21.0	20.9	1
7001	1507	196	-	6.1	47	70	13.82	13.63	19.4	20.6	-1
7153	2606	264	c	5.7	44	58	14.72	14.33	20.6	20.9	1
7170	2444	210	c	7.1	53	72	14.54	14.18	20.6	20.6	0
7222	931	232	c	7.9	113	122	12.25	12.05	19.6	20.5	-1
7279	1978	208	dm	6.7	52	66	14.82	14.40	21.4	21.4	2
7291	226	218	c	6.4	84	105	12.70	12.50	20.2	19.8	1
7301	712	131	c	5.7	45	60	14.92	14.42	21.1	21.0	0
7313	2131	214	c:	5.2	46	59	14.23	13.94	20.4	20.3	0
7321	409	210	c	13.6	125	151	13.42	13.05	20.8	20.9	1
7387	1733	256	c	7.0	52	63	14.27	14.00	20.5	20.4	1
7403	2541	363	c	5.1	68	91	13.08	12.75	18.9	20.7	-2
7459	525	189	c	5.5	52	64	14.22	13.90	20.7	20.6	1
7513	995	280	c	7.2	97	108	12.43	12.27	19.8	19.9	3
7522	1428	310	c	7.2	78	88	12.92	12.74	19.9	20.2	2
7607	4226	278	c	8.4	43	57	15.06	14.71	20.7	20.8	0

Table 1 (*Continued*)

UGC	V_h	W	T	a/b	a_{23}	a_{24}	m_{23}	m_{24}	SB_0	SB_0^d	PI
1	2	3	4	5	6	7	8	9	10	11	12
7617	6972	436	c	6.9	48	72	14.38	14.11	19.8	20.5	-1
7687	1733	144	c	6.5	55	67	14.51	14.07	21.2	21.2	1
7725	1759	151	Ir	4.1	43	59	13.85	13.60	20.3	20.1	0
7774	526	190	c	6.0	57	80	14.15	13.82	21.0	20.5	0
7808	7273	520	b:	4.7	37	74	14.27	13.96	19.5	21.8	-2
7993	4789	366	c	5.8	42	52	14.55	14.30	20.3	20.4	0
7999	4761	442	c:	5.4	51	64	13.37	13.25	19.2	19.4	0
8025	6316	513	b	5.1	47	58	13.50	13.37	19.1	19.4	0
8146	669	162	c	6.1	69	89	13.85	13.46	20.6	20.7	0
8286	407	179	c	7.6	126	148	12.28	12.05	20.4	20.4	2
8463	4647	-	b	4.8	58	69	12.78	12.68	19.1	19.2	1
9115	2049	256	bc	5.2	50	61	13.27	13.11	19.5	19.4	2
9127	2883	570	c	8.5	125	173	12.05	11.87	19.6	19.6	0
9242	1440	187	c	11.6	93	125	14.09	13.65	21.0	21.1	1
9249	1365	147	dm	6.1	45	64	14.96	14.51	21.3	21.0	0
9422	3310	314	c	8.5	55	66	14.21	13.98	20.4	20.6	3
9431	2237	330	c	6.1	69	83	13.20	12.96	19.5	20.0	1
9556	2292	230	c:	4.5	21	29	15.09	14.90	20.1	23.1	-3:
9568	2138	418	b	6.2	79	89	12.66	12.51	19.6	21.0	-1:
9760	2015	144	c	6.0	35	63	15.86	15.03	21.6	21.6	0
9780	5178	335	c	7.1	56	64	14.40	14.09	20.3	20.8	0:
9856	2491	218	c	7.2	42	63	15.15	14.68	20.7	21.0	0
9948	2612	-	bc	6.9	78	88	12.60	12.43	19.1	19.6	2
9977	1912	247	c	7.3	73	96	14.04	13.60	20.8	21.3	1:
10227	9026	600	c	6.9	57	70	14.16	13.89	19.8	20.7	-1
10288	2045	352	c	7.8	96	119	13.47	13.01	20.4	20.5	0
10297	2306	224	-	4.4	38	60	14.55	14.10	20.4	20.4	0
11132	2828	339	b	4.4	40	53	14.20	13.94	19.9	20.0	0
11230	7103	400	c	5.1	31	54	15.12	14.68	20.4	21.6	-1
11301	-	-	-	5.8	59	80	13.67	13.42	18.6	20.9	-2
11394	4236	365	c	6.8	51	66	14.38	14.09	20.2	20.5	1
11411	-	-	-	5.4	43	59	14.75	14.38	20.4	21.1	-1
11838	3478	250	c	6.7	47	60	14.58	14.28	20.5	20.6	1
11841	5989	535	dm	7.5	58	87	13.98	13.70	18.7	21.1	-2
11859	3014	306	b	5.6	31	54	14.79	14.30	20.2	21.6	-1
11893	5564	619	c	6.0	52	73	13.82	13.60	19.5	20.4	-1

Table 1 (*Continued*)

UGC	V_h	W	T	a/b	a_{23}	a_{24}	m_{23}	m_{24}	SB_0	SB_0^d	PI
1	2	3	4	5	6	7	8	9	10	11	12
11964	1399	170	c	6.3	40	54	15.42	14.88	21.4	21.3	1
11994	4872	404	bc	5.1	46	58	13.40	13.22	19.4	19.2	0
12001	4269	534	b	6.1	59	67	13.25	13.10	19.5	20.1	-1:
12190	7263	577	c	6.2	50	60	13.89	13.70	19.5	20.1	-1:
12281	2567	260	dm	9.5	86	102	13.88	13.56	21.0	20.3	1
12411	8656	571	m:	6.0	44	52	14.01	13.87	19.7	19.8	0:
12423	4838	486	c	6.2	62	91	13.60	13.34	19.4	20.6	-1
12430	3676	225	c	6.4	55	66	13.99	13.81	20.6	20.4	0:
12452	4960	314	c	5.3	43	59	14.38	14.12	19.4	20.5	-1
12506	2385	345	c	5.4	50	76	13.87	13.58	19.5	20.8	-1
12693	4952	220	c	5.1	26	45	15.39	14.99	20.8	20.9	0
12900	6803	458	c	6.0	45	56	14.50	14.24	20.3	20.5	0

U711. A distortion from a bright star. The luminosity profile is measured only for the western side of the galaxy.
U1400. A bright star at the center. The galaxy aspect ratio does not satisfy the criterion of the FGC-catalogue (Karachentsev *et al.*, 1993). A background distortion from a bright star at the north.
U1650. A very faint external disk.
U3365. The aspect ratio $a/b = 8.0$ in the UGC is overestimated. It does not satisfy the FGC criterion.
U3425. Dissatisfying the FGC criterion.
U3597. Dissatisfying the FGC criterion.
U3697. Strong distortions at both ends of the galaxy, an integral-like shape.
U4043. The luminosity profile in the I-band obtained by Freudling (1990).
U4257. In contact with a round galaxy at the south.
U4259. A star seen in projection near the centre. Dissatisfying the FGC criterion.
U4277. See also the luminosity profile in Freudling (1990).
U4278. A bright star at the east. Another star is projected onto the northern side of the galaxy.
U4550. Reflection of a bright star on the southern side of the galaxy.
U4704. Irregular brightness distribution in the central region.
U4719. A compact galaxy near the southern end. A bright star reflection is projected at the 1 arc minute distance to the north.
U4961. An irregular central region. A companion in contact on the southern side.
U5452. Dissatisfying the FGC criterion.
U5459. Integral parameters are unreliable due to a bright star on the east.
U5495. A faint red halo.
U5662. The luminisoty profile of a "disk + disk" type.
U6774. A star is projected on to the northern side.
U7170. An integral-like shape.
U7222. The southern side of the image is crossed by a defect CCD-column. The galaxy has a very faint external disk beyond the CCD frame.
U7301. The integral parameters have been measured unreliably due to variable atmospheric conditions.
U7403. A strongly distorted background due to the bright star reflection on the east.
U7513. An irregular brightness distribution near the centre.
U7617. The western side with a sign of tidal distortion.
U7687. A background distortion at the south due to a bright star.
U7725. Dissatisfying the FGC criterion.
U7993. See also the luminosity profile in Freudling (1990).
U7999. I-band profile by Freudling (1990).
U8463. Dissatisfying the FGC criterion.
U9115. A member of a physical pair. Dissatisfying the FGC.
U9127. See the profile in Freudling (1990).
U9422. Background distortion due to a bright star to the north.
U9556. A very faint external disk.
U9760. A star is seen in projection near the center. A background distortion from a bright star to the north.
U9856. Irregular brightness distribution in the central region.
U9948. Dissatisfying the FGC.
U10227. Background distortion due to a bright star to the south. See the luminosity profile in Freudling (1990).

(*Table 1 Notes continued*)

U10297. Dissatisfying the FGC.
U11132. Dissatisfying the FGC.
U11301. Projections of many Milky Way stars are projected.
U11394. Seen at a low galactic latitude.
U11411A. According to the PGC, the galaxy coordinates are RA = $19^h10^m08^s$, D = +60°07′.
U11838. A star reflection is projected onto the southern end.
U11841. A star is projected near the center. A faint external disk.
U11859. The southern side is cut by the CCD-frame.
U11893. Numerous stars projections.
U11994. The NE-side background is distorted by a bright star reflection.
U12001. Background distortion due to a bright star reflection. Dissatisfying the FGC criterion.
U12190. The background is distorted by a star reflection.
U12281. Irregular brightness distribution near the center.
U12411. Brightness distribution on the northern side is strongly affected by a bright star.
U12430. Two brightness peaks in the central region.
U12506. See also the luminosity profile in Freudling (1990).

6.9×5.2 arc minutes with the angular resolution of $0''.61 \times 0''.81$. Detailed description of the CCD-device can be found in Borisenko *et al.* (1990). All the objects were observed in the red pass band, close to the R'-system of Cousins (1976) with $\lambda_{\mathrm{eff}} = 6500$ A. A typical exposure time was 500 seconds. As photometric standards, we used the aperture magnitudes of galaxies from the catalogue of de Vaucouleurs and Longo (1988).

We observed 121 galaxies from the aforementioned sample. Four galaxies (UGC 7322, 7694, 7772, and 9801) had been excluded due to their large dimensions, $a > 10$ arc minutes. The data for UGC 10561 were contaminated by a neighbouring bright star. The remaining galaxies are listed in Table 1.

3. DATA REDUCTION

After recording on a magnetic tape in the FITS format, the obtained CCD images were subjected to a preliminary standard processing, i.e. dark frame subtraction, flat field correction, and some bad-columns cosmetic. Subsequent procedures of the data processing were made with a ROBOTRON CM 1630 minicomputer using the Rozhen software package (Georgiev, 1991) as well as the Babelsberg one (Richter, Lorenz, 1989). The CCD-frames were also corrected for the scale anisotropy at the 4:3 rate. After cleaning the frames for bright-star images and cosmic events filtering, we carried out the small-scale smoothing and linear correction of the sky background level.

At the photometric stage, we used a software for the zero-point determination on the photoelectric aperture photometry data. Then we determined for each object the surface brightness, integral magnitude, axial ratio, and position angle of the major axis as functions of the distance from the galactic center. In addition, we obtained for each galaxy photometric profiles along the major and minor axes, and the so-called "generalized" profile as proposed by Watanabe (1983). The latter morphological functions will be considered separately. Here we present half-tone images of the flat galaxies as well as their apparent magnitudes and angular diameters, measured at two distinct isophotal levels.

4. RESULTS

In Figure 2 we present fragments of CCD-images obtained for 120 flat galaxies. Each object is shown using 5 grey-scale tones with a step of 0.2 mag. The isophotes between the white and black tones correspond to 25, 24, 23, ... mag. The faintest visible isophote corresponds to 25.8 mag (the sky background is ≈20.5 mag). The UGC number is given at the top of each panel, the 30″-bar gives a scale, and arrows indicate the north and east directions.

During observations we used nights with different seeing. Its average value was 3-4″; the difference in seeing, however, slightly affected the measured parameters of larger galaxies. An additional decrease in the resolution of the presented images is caused by a specific property of the CCD with the surface charge transfer, and by a small-scale smoothing procedure. In some CCD images (say, UGC 507 and 7222) one can see traces of imperfect correction of bad columns. Brightness distributions for the flat galaxies is shown in Figure 3. The horizontal

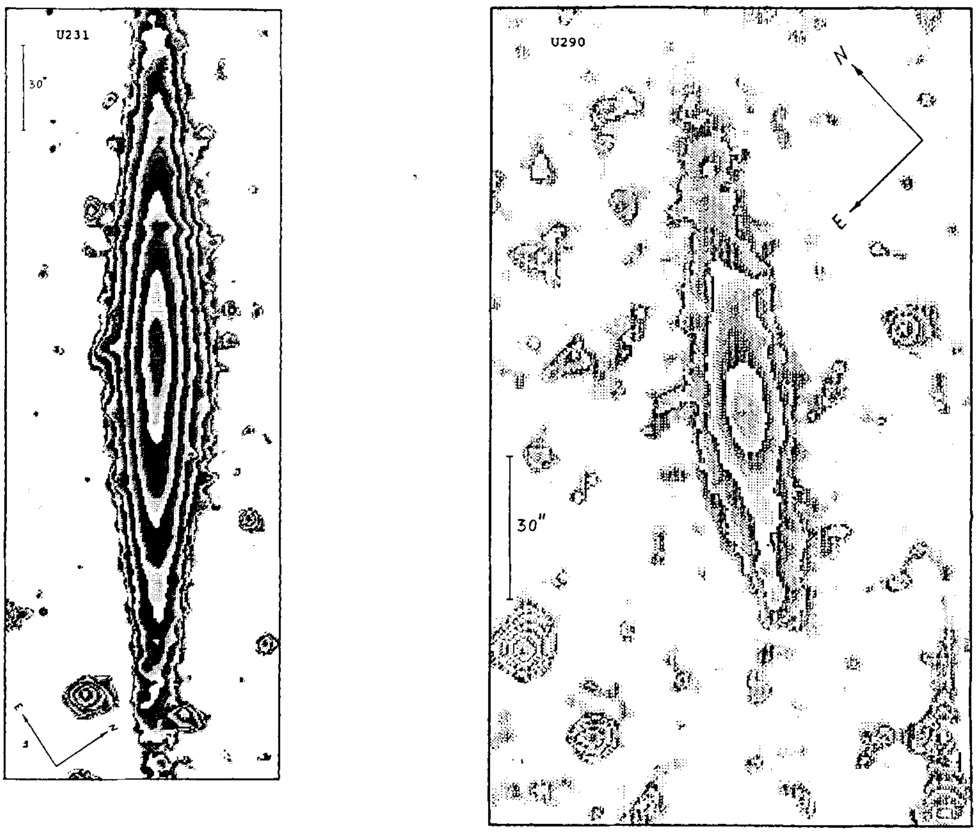

Figure 2 Grey-scale maps of 120 flat galaxies. The CCD-frames were obtained in the R'-passband on the 6-meter telescope with the exposure time of 400–600 seconds. The gray-scale grades correspond to 25, 24, 23, . . . mag/arc second^2; the faintest isophote corresponds to 25.8 mag/arc second^2. The UGC number of the galaxy is indicated at the top, the scale and the north and east directions are shown by the bar and arrows, respectively.

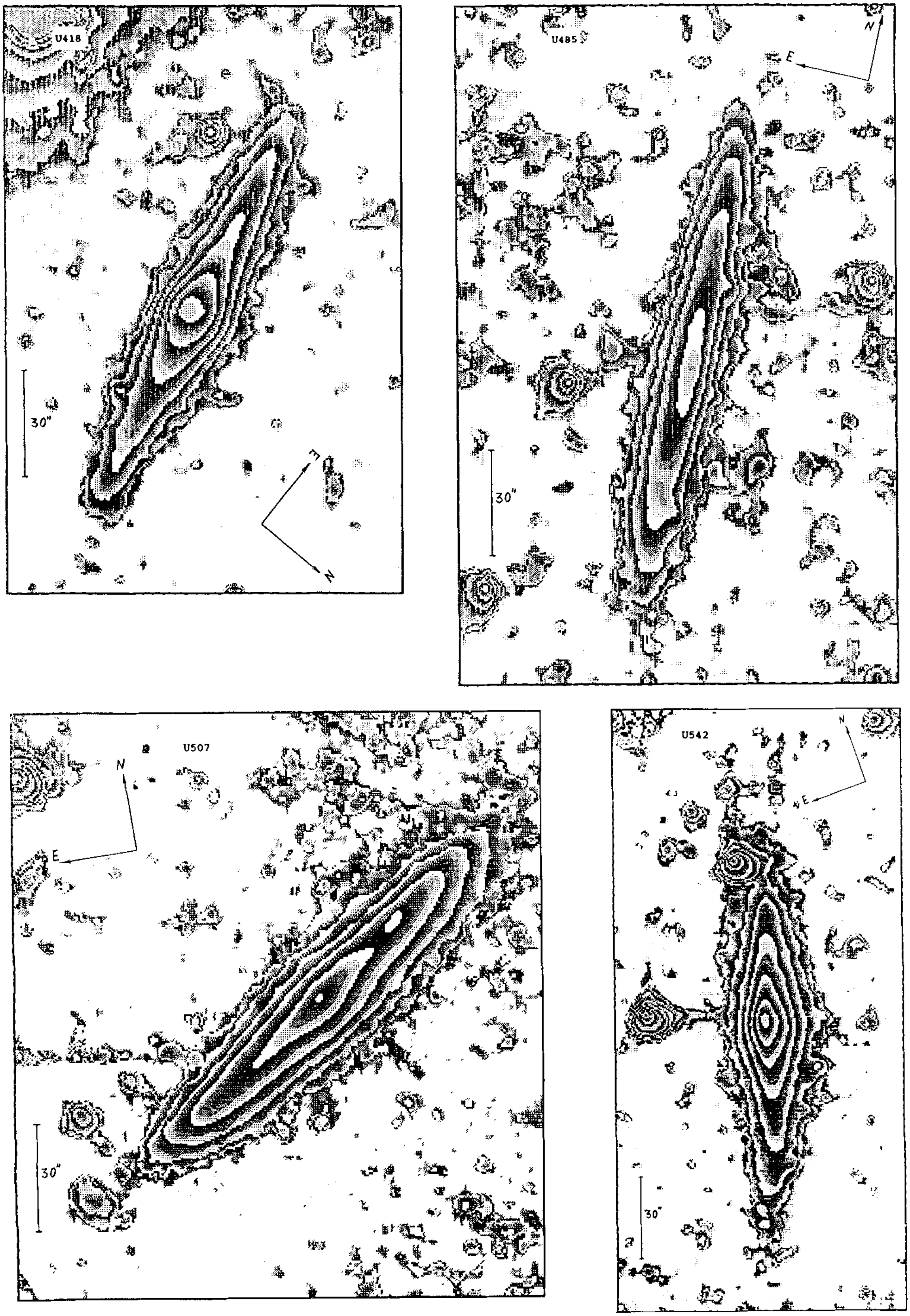

Figure 2 (*Continued*)

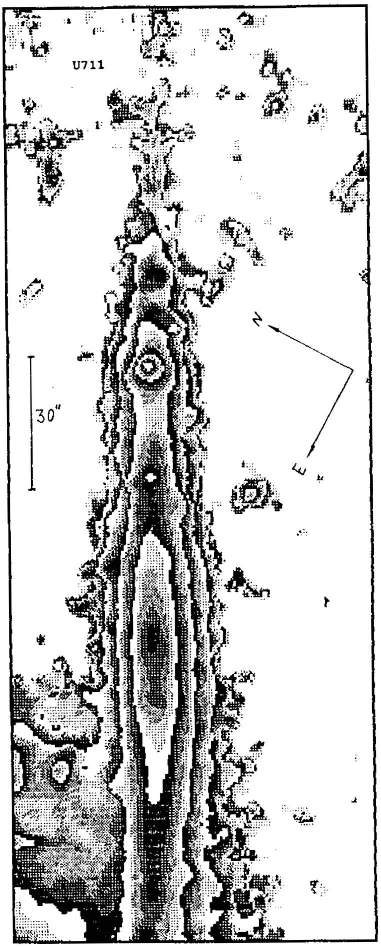

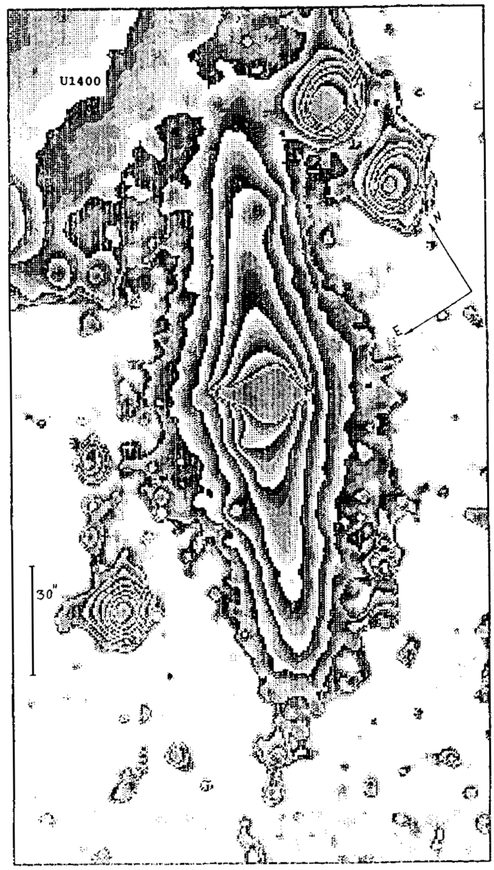

Figure 2 (*Continued*)

axis is the angular distance measured in arc seconds from the center of the galaxy along the major axis. The vertical axis is the averaged surface brightness in mag. per square seconds, averaged over the positional angles. For several galaxies (UGC 231, 542, etc.) we present luminosity profiles obtained during several nights. Their comparison allows to estimate the photometric error and to assess the reality of one or another feature of the surface brightness profile.

In Table 1 we compile some basic parameters for our sample galaxies:

(1) the galaxy number in the UGC catalogue;

(2) the radial velocity in km/s relative to the Sun;

(3) the 21 cm FWHM linewidth in km/s. The data are taken from the survey of Bottinelli *et al.* (1990) with supplements from Huchtmeier and Richter (1989) and Haynes and Giovanelli (1992);

(4) the morphological type according to the UGC (Nilson, 1973);

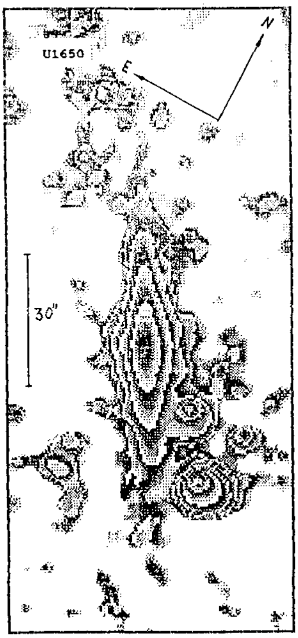

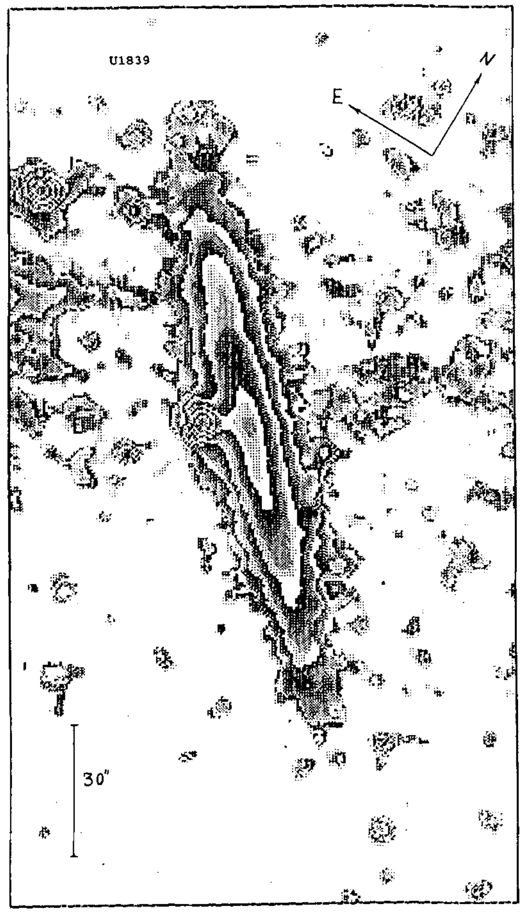

Figure 2 (*Continued*)

(5) the maximal aspect ratio according to our photometric data;

(6) and (7) the galaxy angular radius along the major axis at two surface brightness levels, 23 mag/arc second^2 and 24 mag/arc second^2;

(8) and (9) the apparent red (R') magnitude within the isophotes of 23 and 24 mag/arc second^2;

(10) the observed surface brightness at the center of the galaxy;

(11) the surface brightness of the disk, extrapolated to the center;

(12) the "profile index", PI, which gives the degree of deviation of the observed profile from an ideal exponential dependence (corresponding to PI = 0). Positive values of PI correspond to a curved profile with a central depression, negative ones describe profiles with a central peak (i.e., the bulge). The value of PI is equal to the maximal difference between the observed surface brightness and the expected exponential one, measured in the apparent magnitudes (for $SB < 25$ mag./arc second^2). The cases of the unrealiable classification are indicated by the colon.

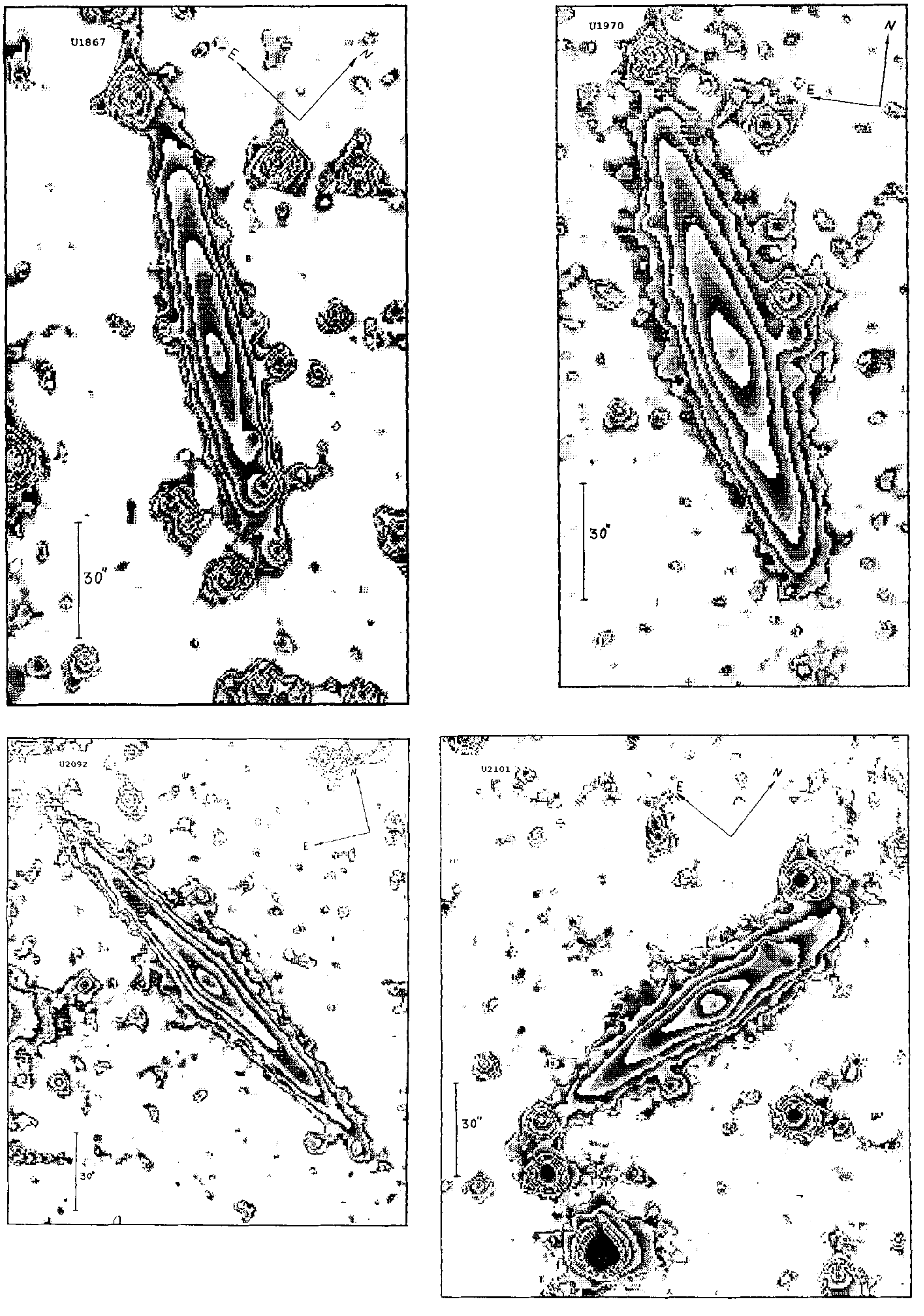

Figure 2 (*Continued*)

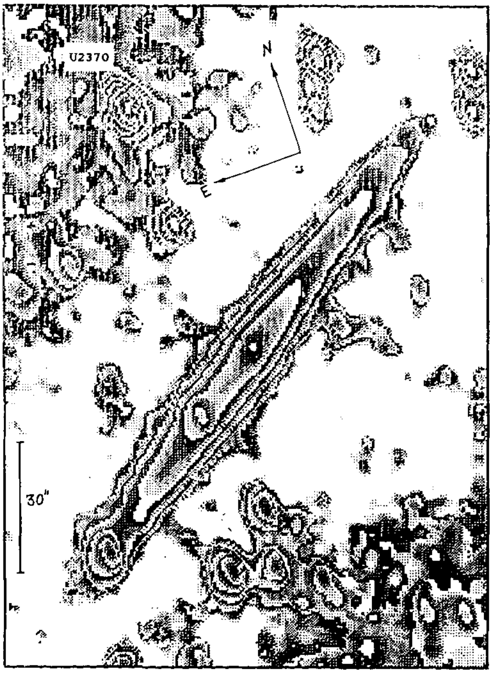

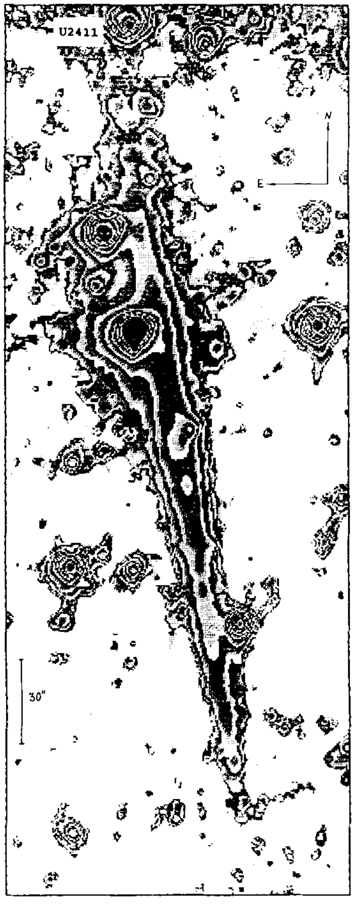

Figure 2 (*Continued*)

Notes to Table 1 contain comments on some features of the flat galaxies, some of them refer to the images and profiles given in Figure 2 and Figure 3.

5. DISCUSSION

Comparison of the CCD-frames obtained for the same galaxy at different times yields the following estimate of the average squared scatter of the apparent total magnitude: $\sigma(m^R_{\rm CCD}) = 0\overset{m}{.}11$. This includes variations of the observation conditions and also possible differences in the photometric zero-point when different standards were used.

Figure 4 shows the relation between red and blue apparent magnitudes for our sample galaxies. The blue magnitudes are taken from the CGCG (Zwicky *et al.*, 1961–1968) with the correction described in PGC (Patural *et al.*, 1989). The red CCD magnitudes correspond to the isophotal level of 24 mag/arc second^2. After

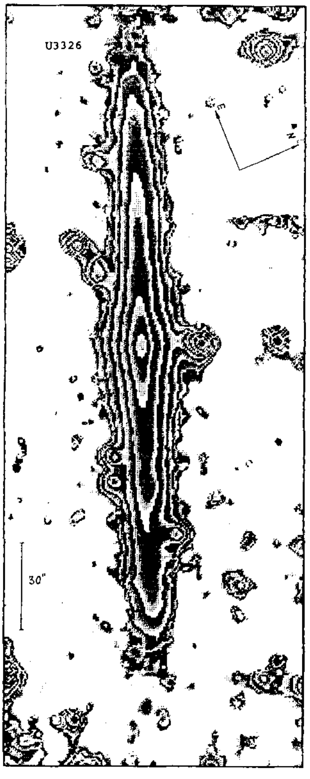

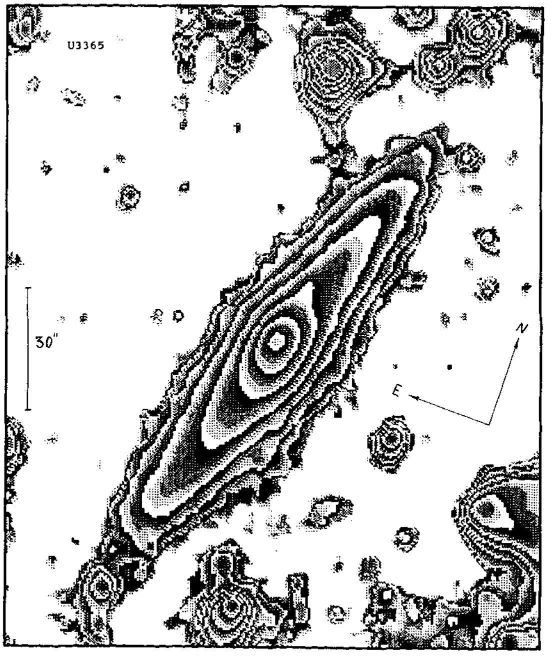

Figure 2 (*Continued*)

exclusion of 8 galaxies at low galactic latitudes $|b| < 15°$ (marked by open circles), we obtained the mean magnitude difference as

$$\langle m^R_{\rm CCD} \rangle = m^B_{\rm PGC} - 1\overset{m}{.}0,$$

with the standard deviation $\sigma_m = 0\overset{m}{.}54$. As expected, the agreement between blue and red magnitudes for edge-on galaxies is somewhat worse than usual ($\sim 0\overset{m}{.}35$). Two reasons easily explain this: a special feature of Zwicky's "Schraffierkasseta" photometric method and variations of light absorption in the galaxies.

The red-light diameters from UGC display a rather tight correlation with the red-light CCD diameters (see Figure 5). The standard deviation with respect to the regression line,

$$\langle \lg a^R_{\rm CCD} \rangle = \lg a^R_{\rm UGC} - 0.05,$$

amounts to 0.06, which equals to $0\overset{m}{.}28$ on the magnitude scale. In other words, the angular diameter of a thin edge-on galaxy is a more reliable (and assessible) distance indicator than its blue apparent magnitude.

Figure 6 demonstrates the correspondence between photometric (CCD) and visual (UGC) estimates of the aspect ratio for flat galaxies. There is no clear relation between these values. Some reasons of that may be proposed. Firstly, the blue-light aspect ratio, a/b, is usually larger than the red-light one owing to the

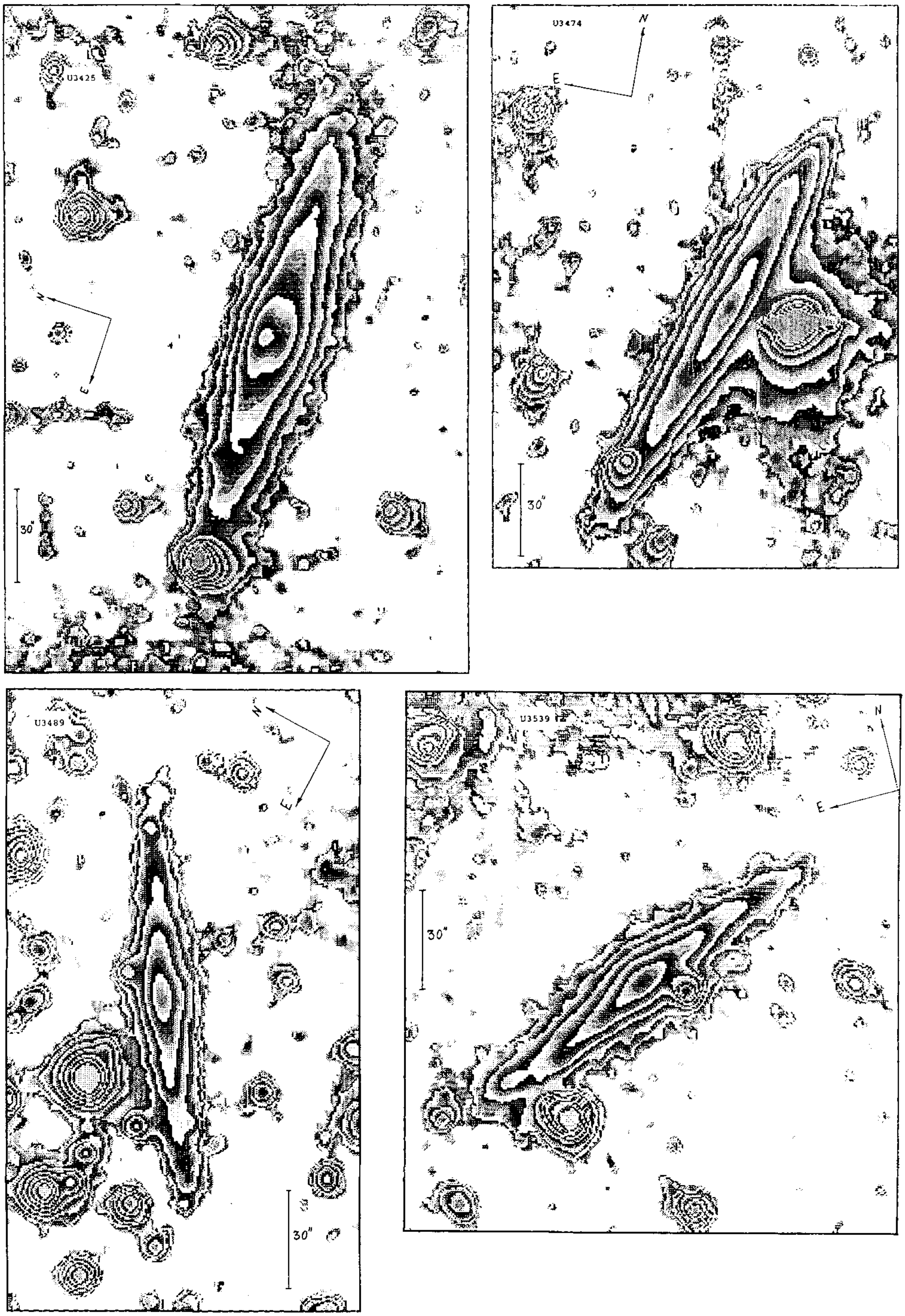

Figure 2 (*Continued*)

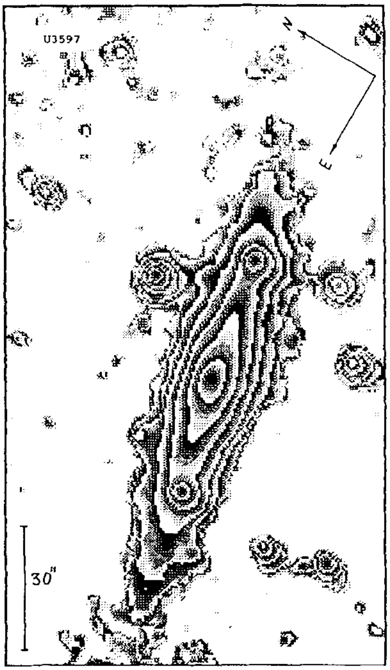

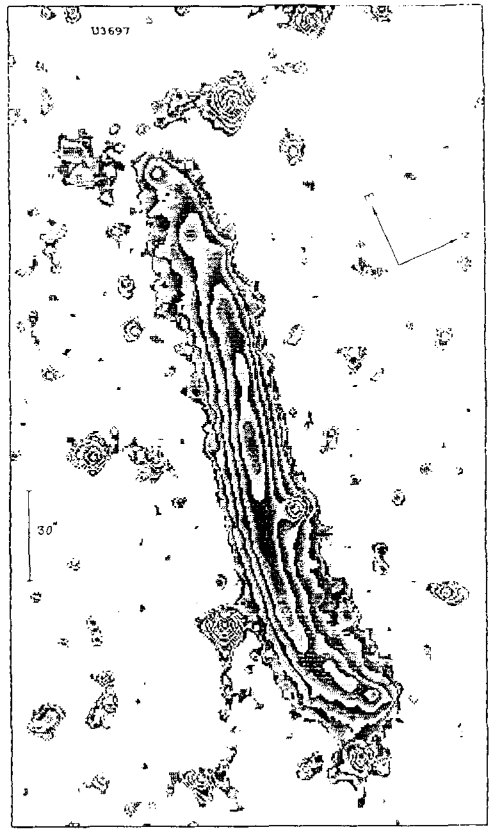

Figure 2 (*Continued*)

bulge-disk color difference. Another reason is a subjective overestimation of any elongated image dimension estimated by eye. The measuring accuracy of the UGC catalogue (0.1 minute of arc) has some significance, especially for the thinnest galaxies. One should bear in mind that the apparent aspect ratio is not constant for some galaxies, being dependent on the surface brightness level.

After excluding several objects (for instance, UGC 2370 and 12900) whose abnormally high aspect ratios have not been confirmed by new measurements (Karachentsev *et al.*, 1993), we obtain the mean difference

$$\langle \lg (a/b)^{B}_{\rm PGC} - \lg (a/b)^{R}_{\rm CCD} \rangle = 0.15.$$

According to our photometric data, the galaxies whose aspect ratio exceeds the maximum value $(a/b) = 15$ are practically absent. The existence of such limit may be of importance for the theory of the origin and evolution of galactic disks.

Inspection of the luminosity profiles in Figure 3 reveals a great variety of their forms. Only one-third of the galaxies have the classical exponential profiles within the accuracy of ± 0.5 mag. Another third of the sample shows the signs of the central peak ($\mathrm{PI} < 0$) caused by the bulge. The remaining galaxies have positive PI, i.e. their profiles indicate either a central depressions or a steep decline at the

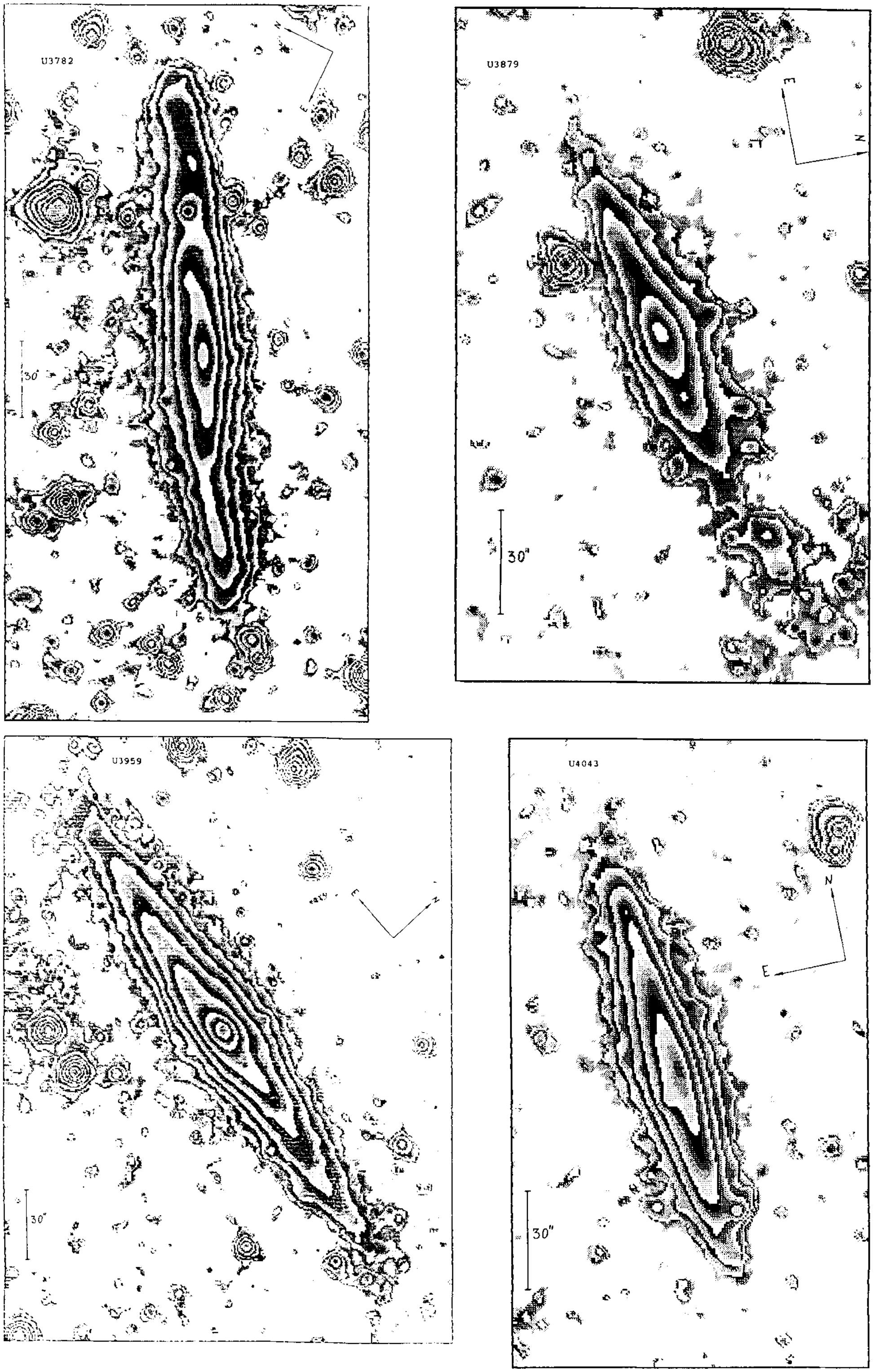

Figure 2 (*Continued*)

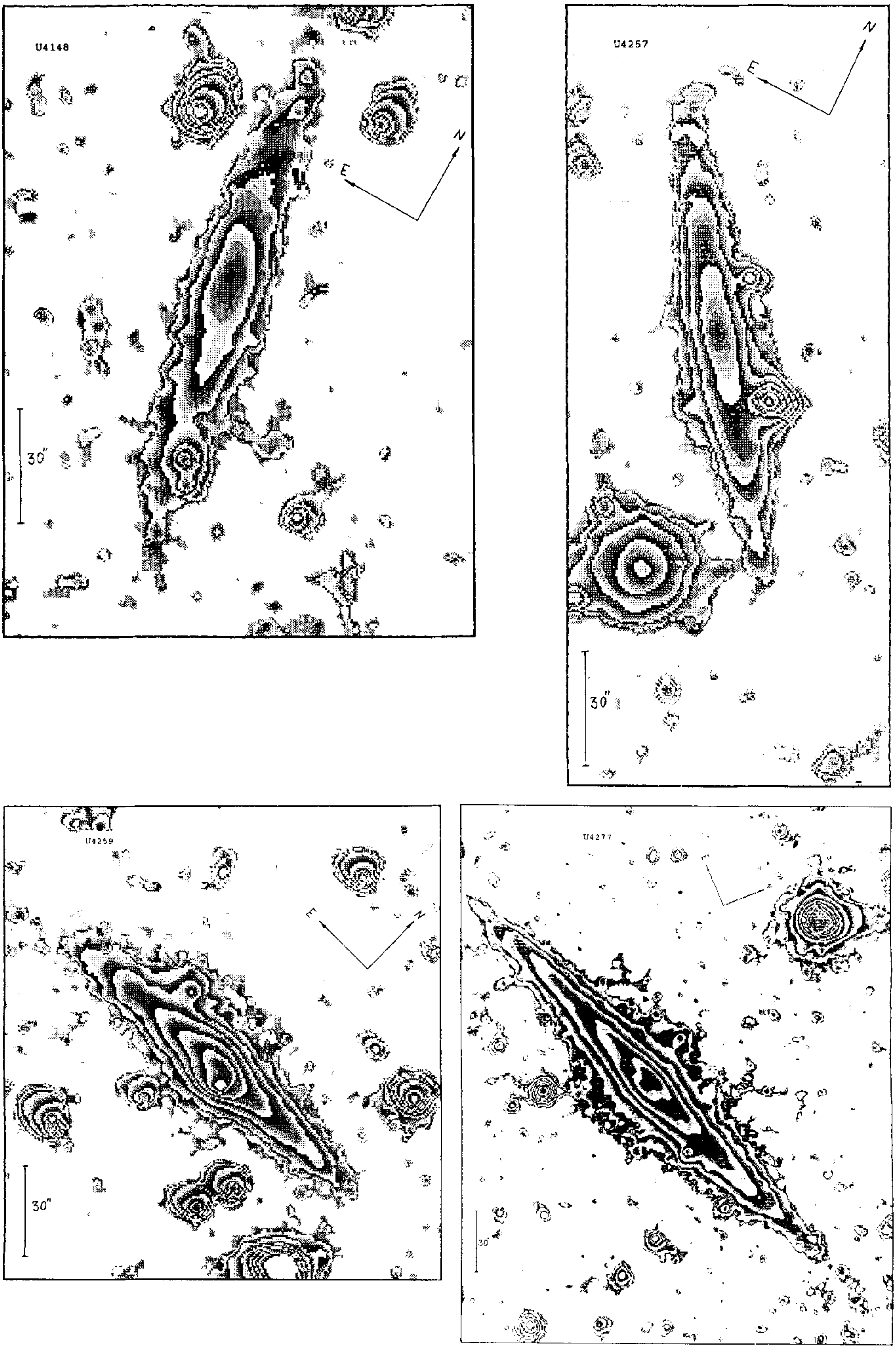

Figure 2 (*Continued*)

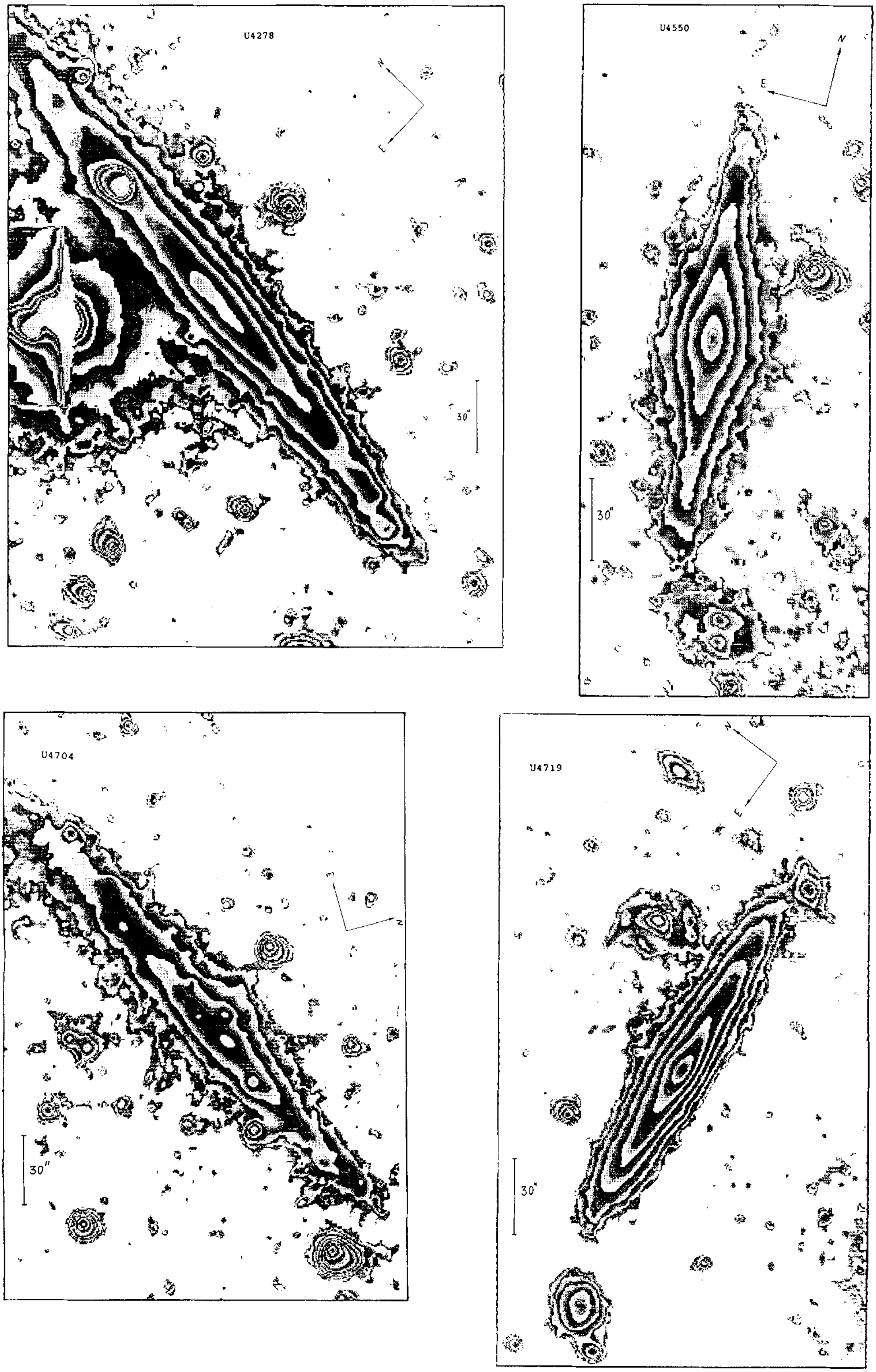

Figure 2 (*Continued*)

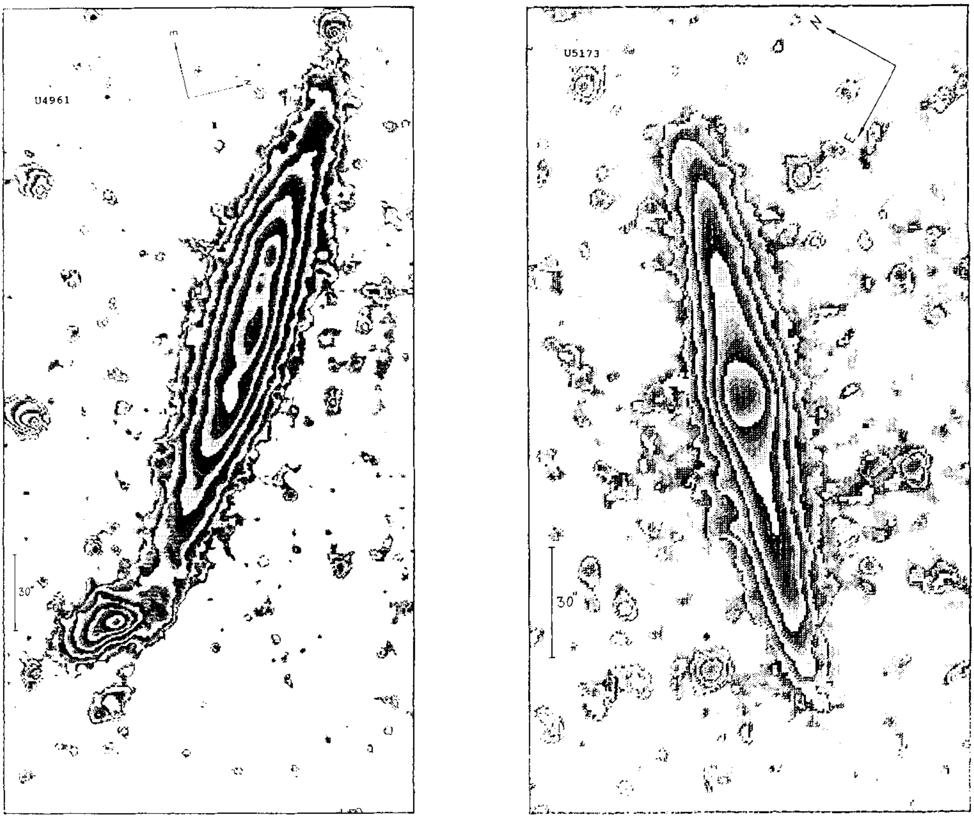

Figure 2 (*Continued*)

disk periphery. In some cases (UGC 5662, 7001, 9556 and 11230) the profile can be fitted by a two-layer structure of the "disk + disk" type.

Comparison of the luminosity profiles for the galaxies observed repeatedly confirms that these features of their profiles are mostly real. Using this subsample we estimated the mean square scatter of the surface brightness at its different levels. The results are presented in Table 2. As one can see, the photometric errors do not strongly distort the intrinsic luminosity profile of a galaxy within the range of SB < 25 mag/arc second^2, i.e. one per cent above the mean night-sky brightness.

The observed variety of luminosity profiles for the flat galaxies may be caused by the following two reasons: a non-uniform structure of their stellar subsystems, as well as a strong variation of the intrinsic absorption along the galactic disk seen edge-on. Valentijn (1990) and Devies (1990) recently presented arguments in favor of the viewpoint that disks of spiral galaxies are opaque, so that only a small fraction of their stellar population light reaches an external observer. In this case the existence of many galaxies showing a central depression in their luminosity profiles should be ascribed to the influence of light absorption.

However, some data disagree with such picture. For instance, Freudling (1990)

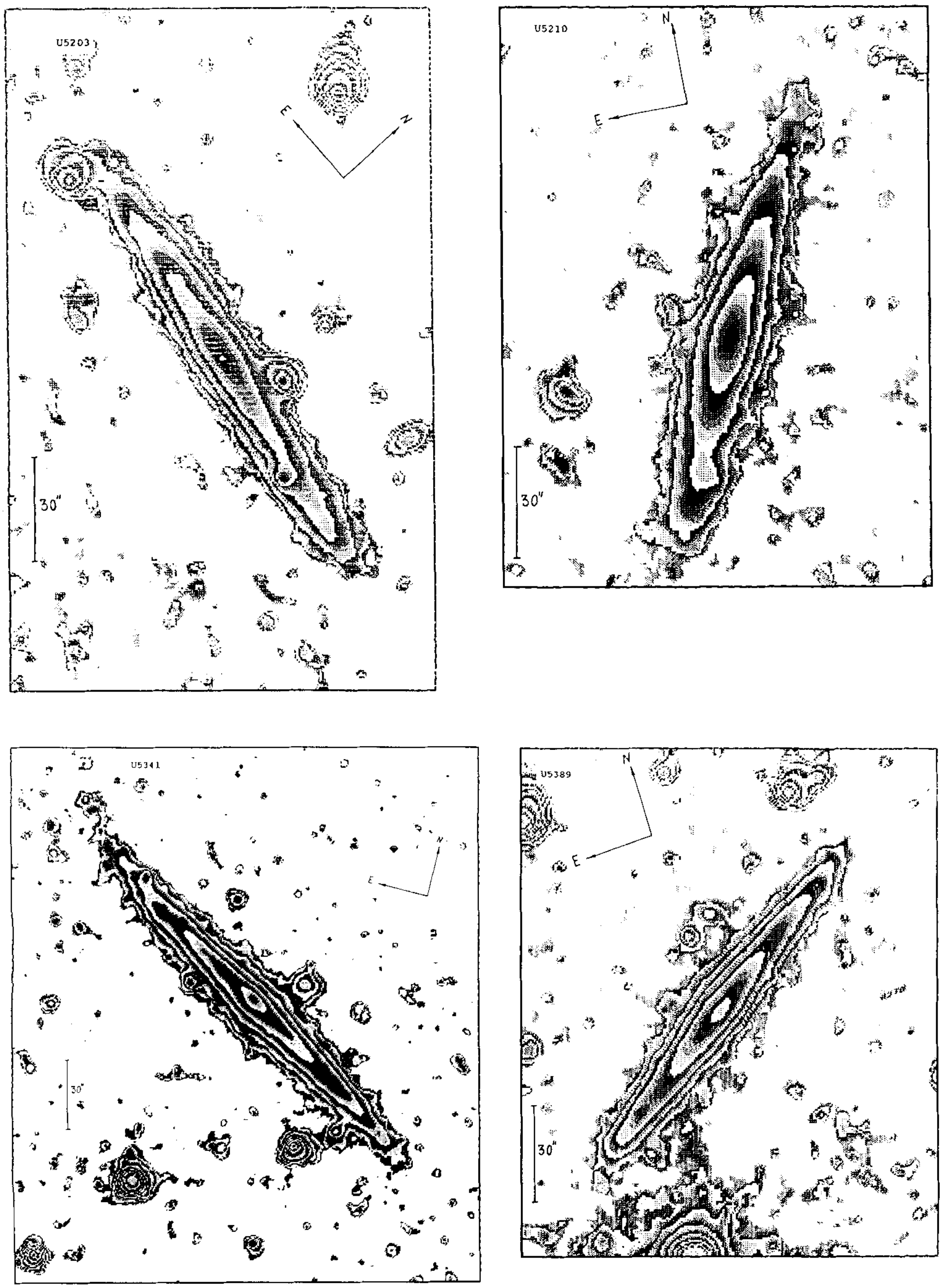

Figure 2 (*Continued*)

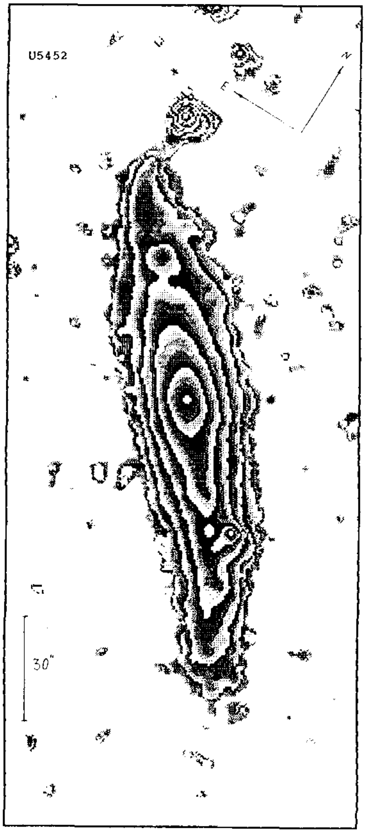

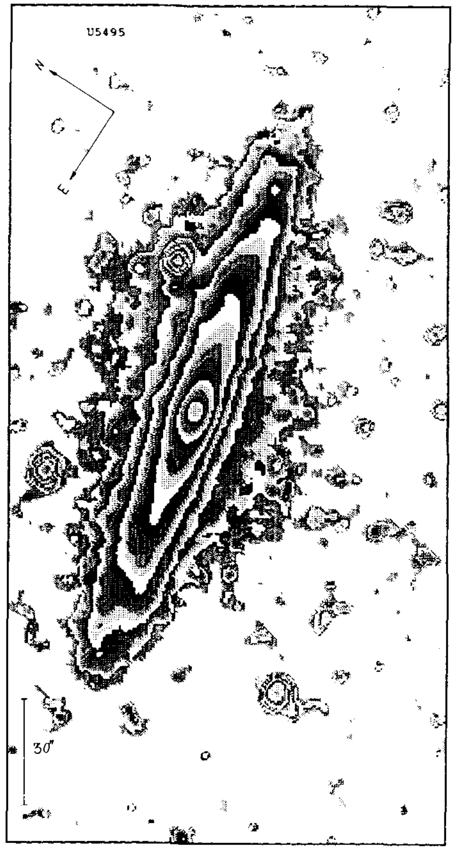

Figure 2 (*Continued*)

carried out CCD-observations and obtained I-passband luminosity profiles for 130 Sc galaxies, inclined at arbitrary angle to the line of sight. Their number distribution over the PI types does not differ essentially from the corresponding distribution for the flat galaxies, irrespectively of the drastic difference in the light passing conditions inside the galaxies of the two samples. Moreover, the total mass-to-total-luminosity ratio of spiral galaxies does not increase but decreases at average with its profile index (Karachentsev, 1991b) as expected in the case of heavyly dusted galaxies.

Figure 7 shows the relation between the amplitude of the inner motions (W_{50}) and the surface brightness at the disk center (SB_0^d) for the flat galaxies. Objects with positive and negative profile indices are indicated by different symbols. One can see from this that the central surface brightness of the disk is apparently independent of the amplitude of the inner motions (or the total lulminosity). However, there is a segregation of the galaxies with different profile indices along the HI linewidth axis: the objects having traces of a bulge occupy the region of larger W_{50} = linewidths. Galaxies with a nearly exponential profile (PI = 0) are distributed over the whole range SB_0^d and W_{50}, being slightly biased towards

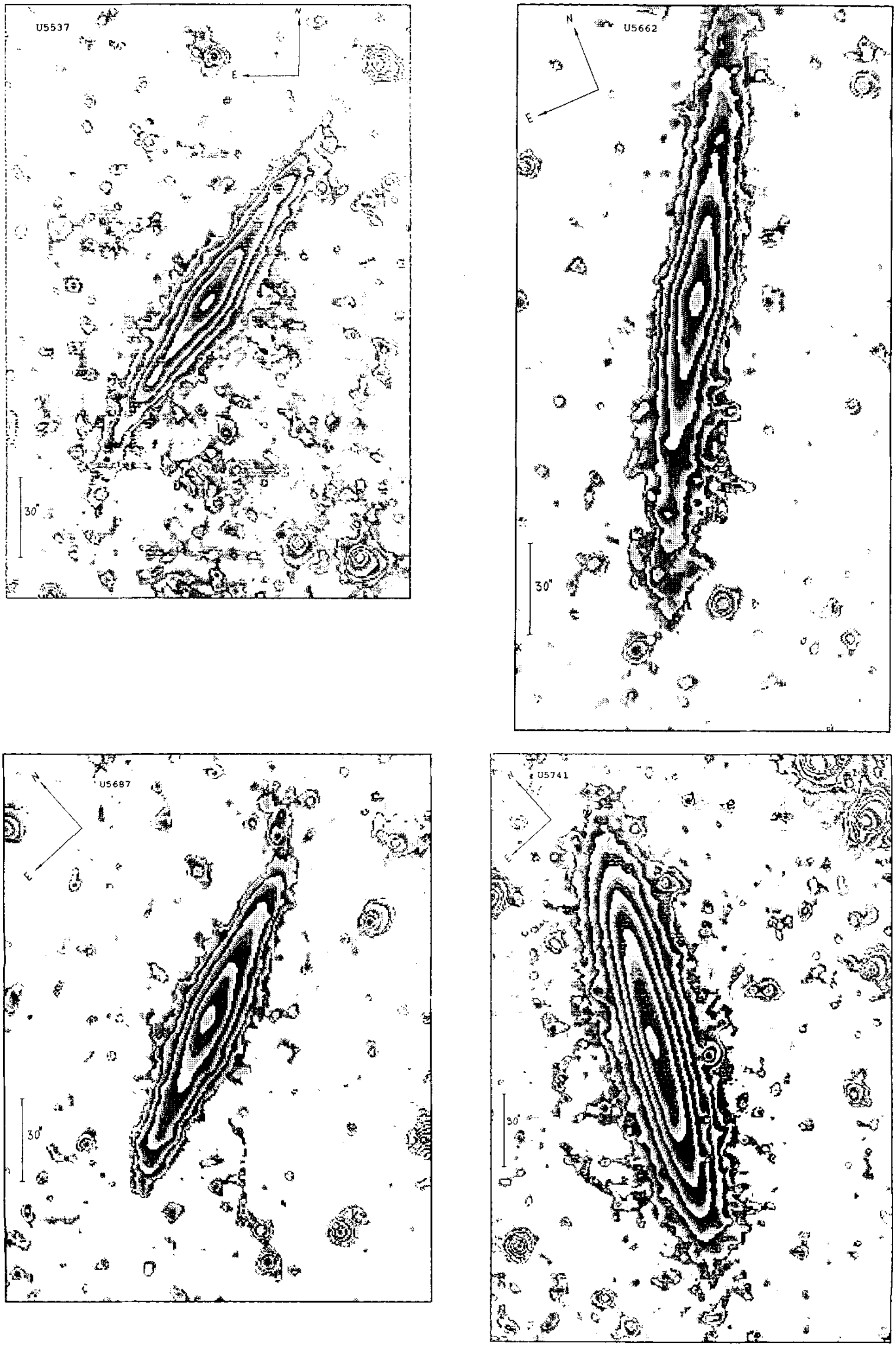

Figure 2 (*Continued*)

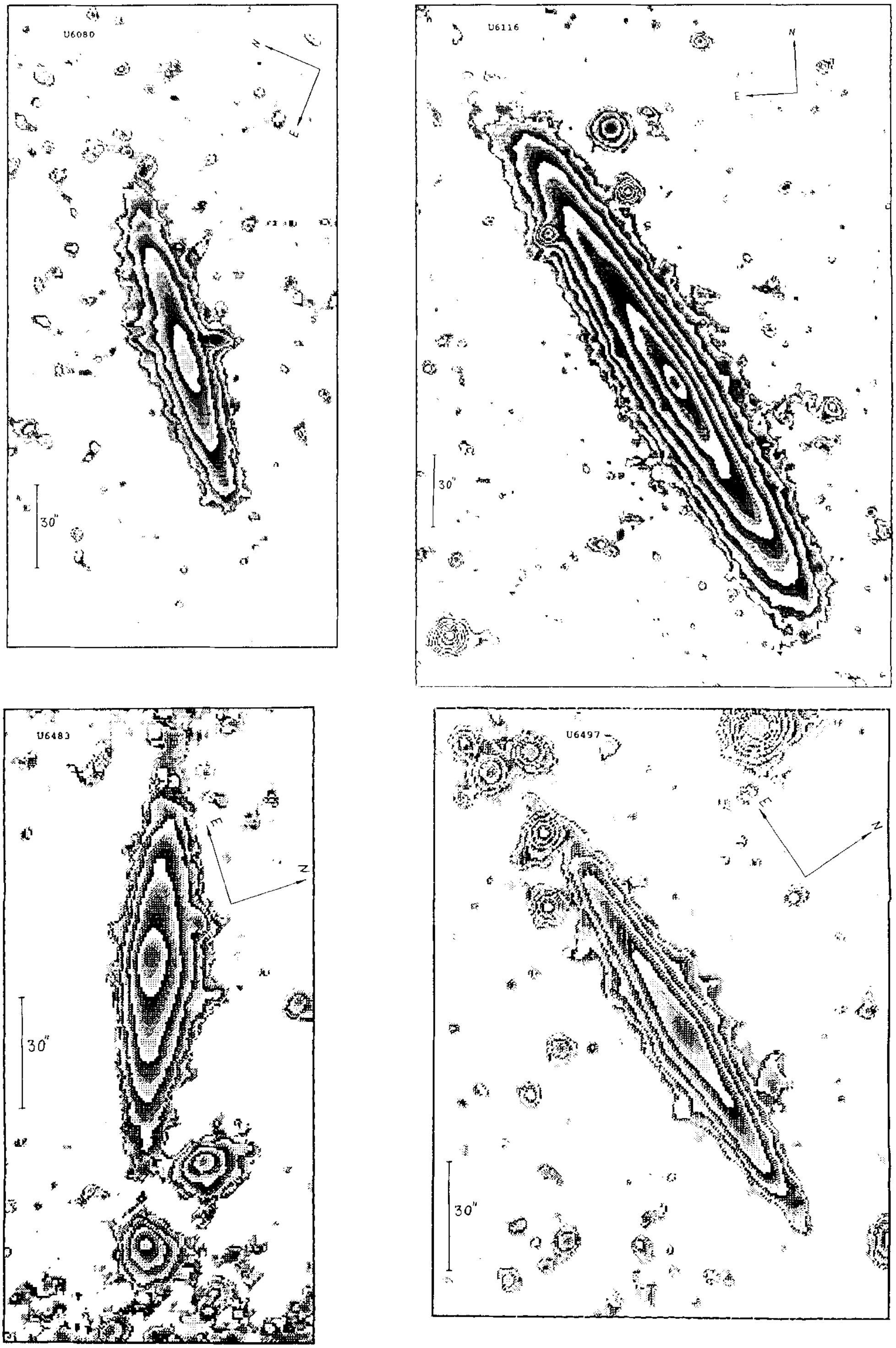

Figure 2 (*Continued*)

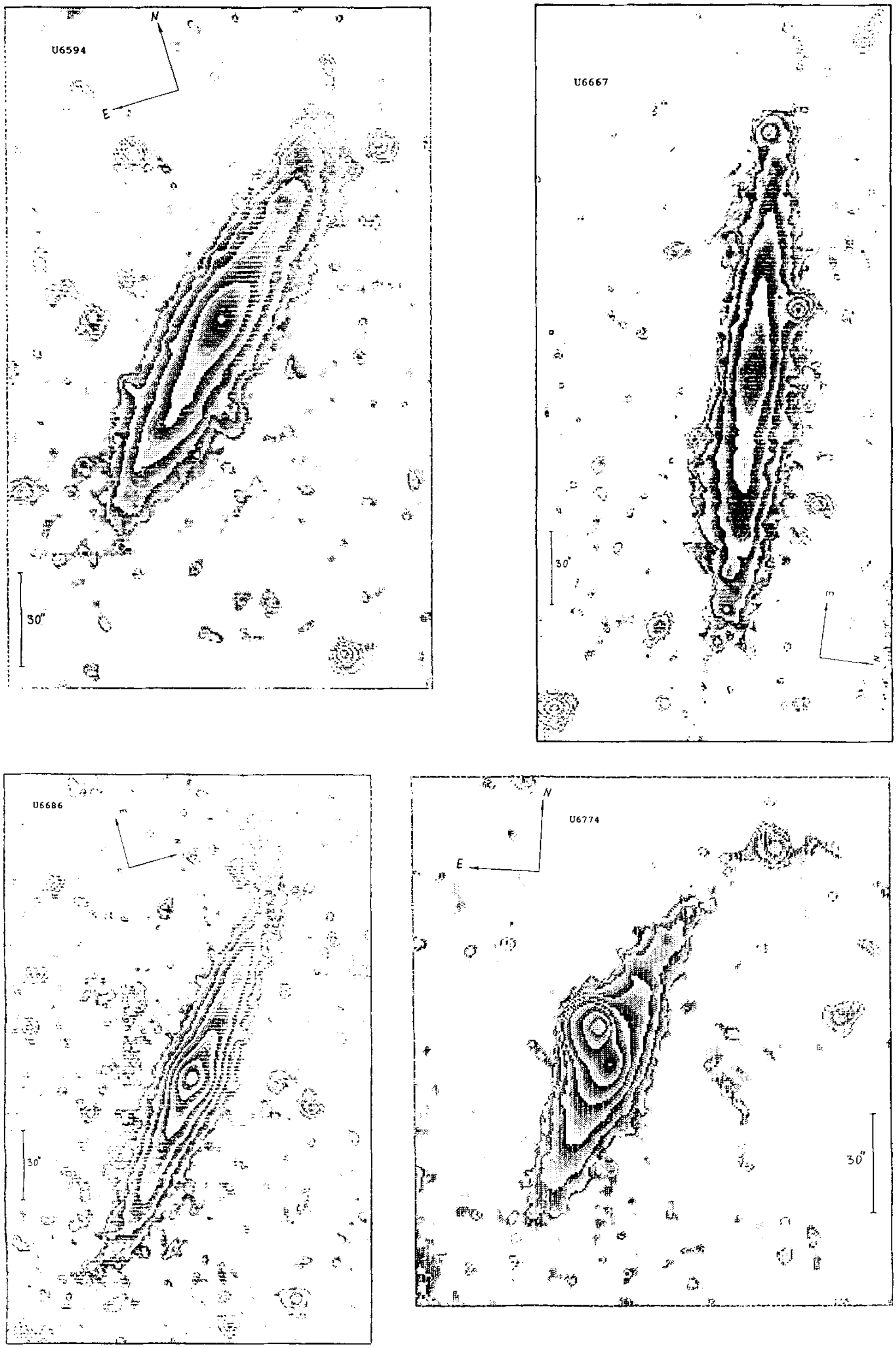

Figure 2 (*Continued*)

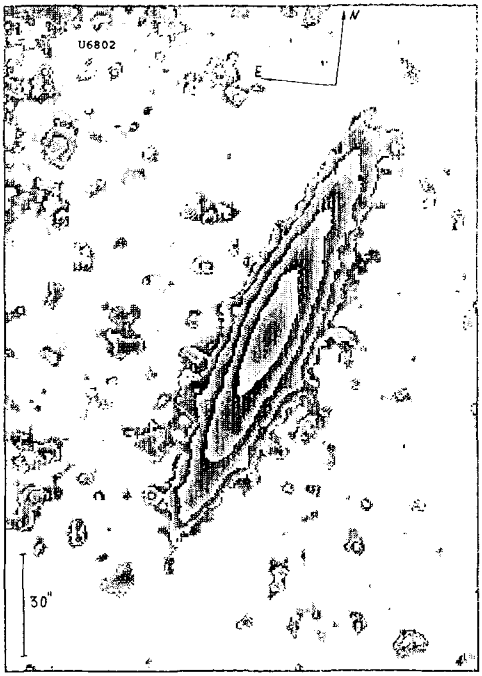

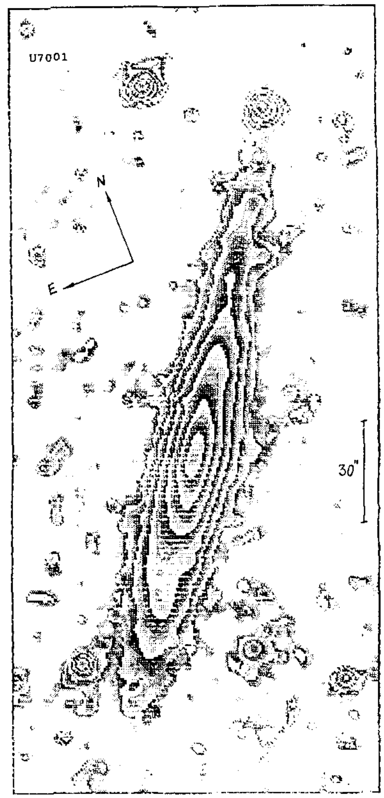

Figure 2 (*Continued*)

dwarf galaxies ($W_{50} < 250$ km/s). The distribution of profiles may be related to the dark matter presence in disk galaxies. In order to explain them one should use observational data on rotation curves of galaxies.

6. CONCLUSIONS

A digital CCD photometry is performed for an almost complete sample of 120 large ($a \geqslant 2$ arc min) spiral galaxies with the apparent aspect ratio $a/b \geqslant 7$. The comparison of the red-light isophotal magnitudes and angular diameters with available catalogue data shows that the red-light angular diameter is a more adequate distance indicator for this type of galaxies.

An apparent axial ratio, a/b determined by the galaxy photometry, turns out to be, as a rule, smaller than its UGC value. Even for the thinnest, according to the UGC, galaxies their aspect ratio does not exceed the limit $(a/b)_{\max} = 15$. The existence of such critical value may be of a great significance for the origin and evolution of disk-like galaxies.

The surface brightness distribution along the radius exhibits a great diversity from one galaxy to another. To describe this quantitatively we propose a

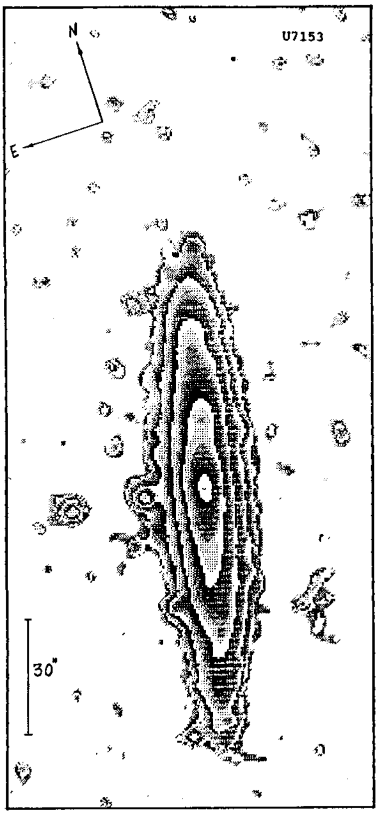

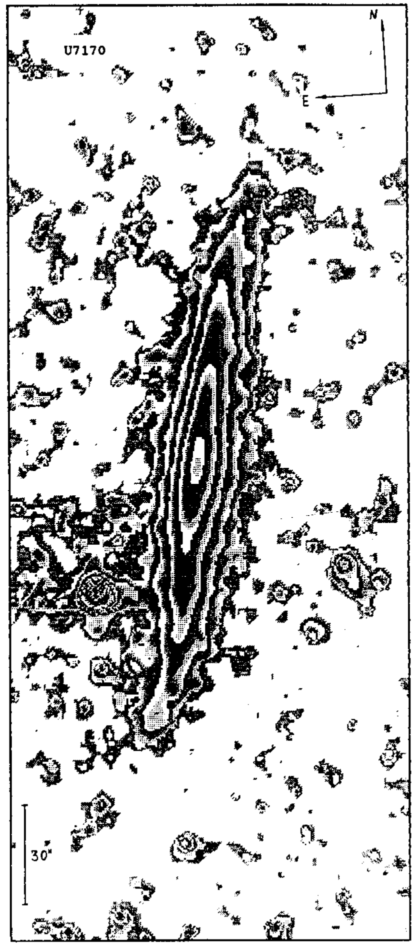

Figure 2 (*Continued*)

one-parameter classification of luminosity profiles according to their deviation from an ideal exponential law. Only one-third of galaxies in our sample have the profiles close to the exponential one.

Approximately the same number distribution of the profile index is found for the sample of 130 arbitrary inclined Sc galaxies whose luminosity profiles have been measured in the *I* band by Freudling (1990). We interpret this as an evidence that the main reason of the observed luminosity profile diversity is most likely a structural difference in their stellar populations rather than the effects of strong internal absorption.

The basic photometric properties of the observed flat galaxies are presented in Table 1. These new data on isophotal diameters, central disk brightness, profile indices and other parameters open a new field for analysis of the effects which affect the accuracy of direct estimations of the distances to spiral galaxies.

One of the authors (I.K.) thanks M. Haynes and R. Giovanelli who provided us their 21 cm data prior to publication.

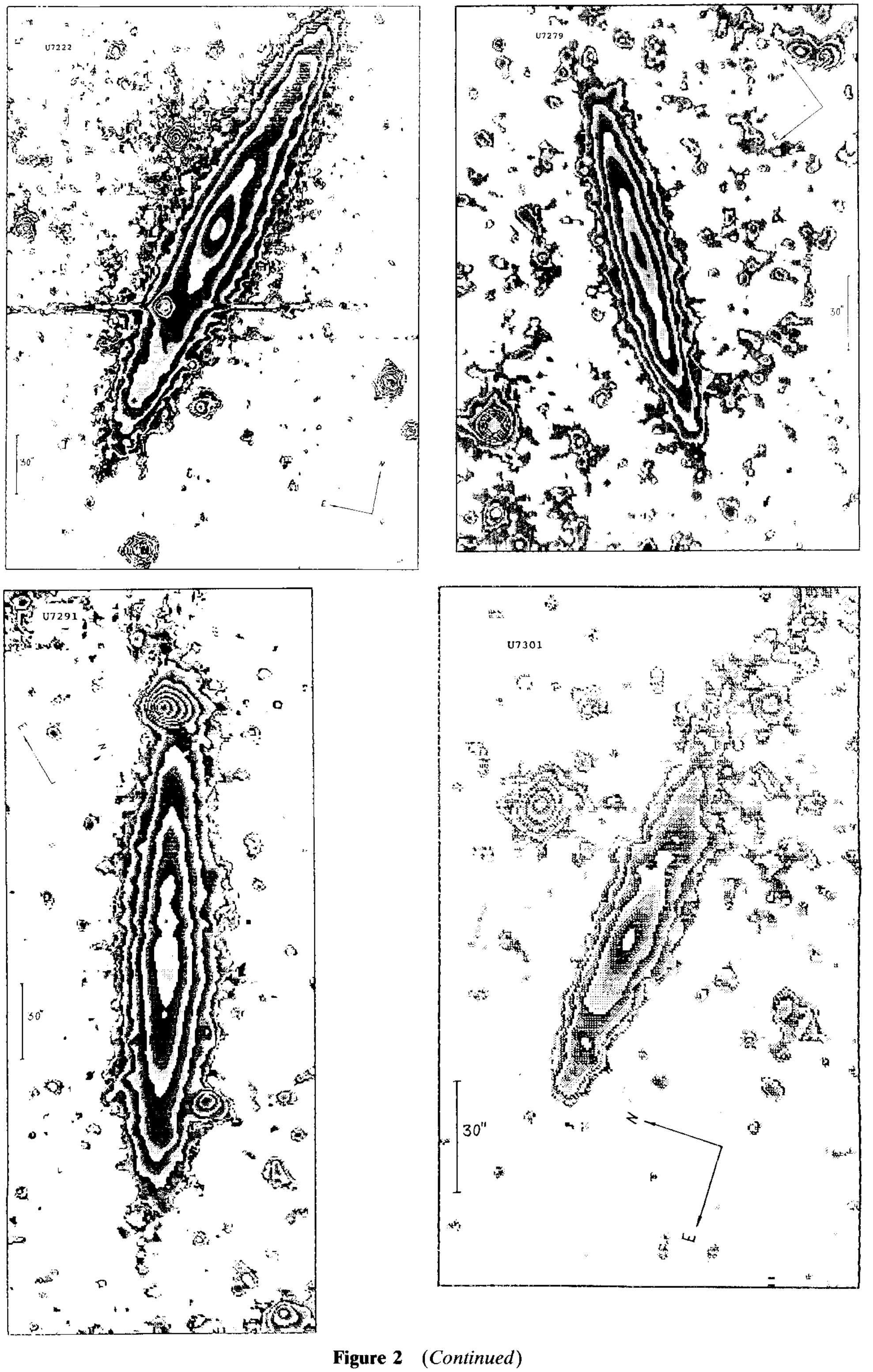

Figure 2 (*Continued*)

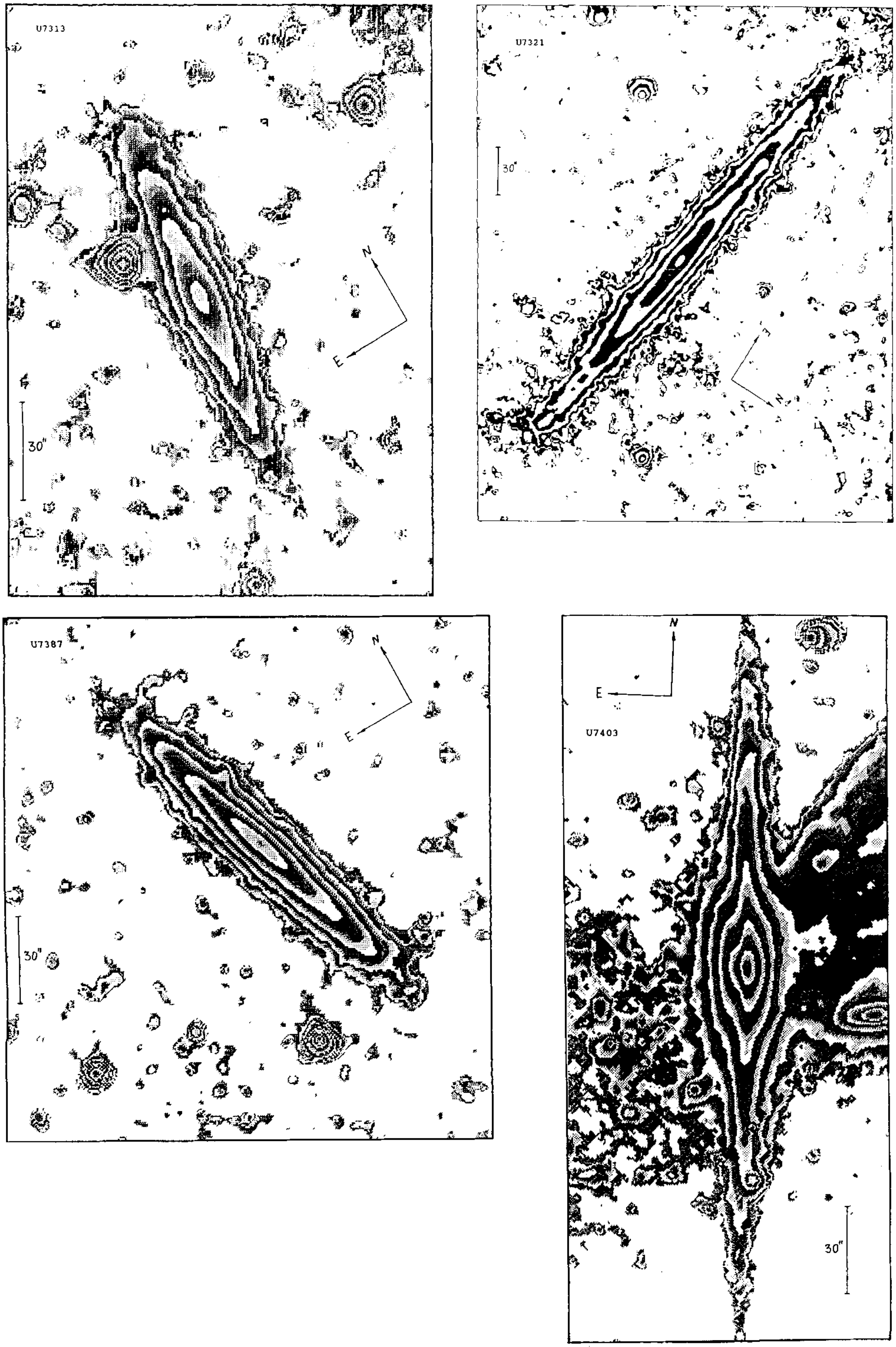

Figure 2 (*Continued*)

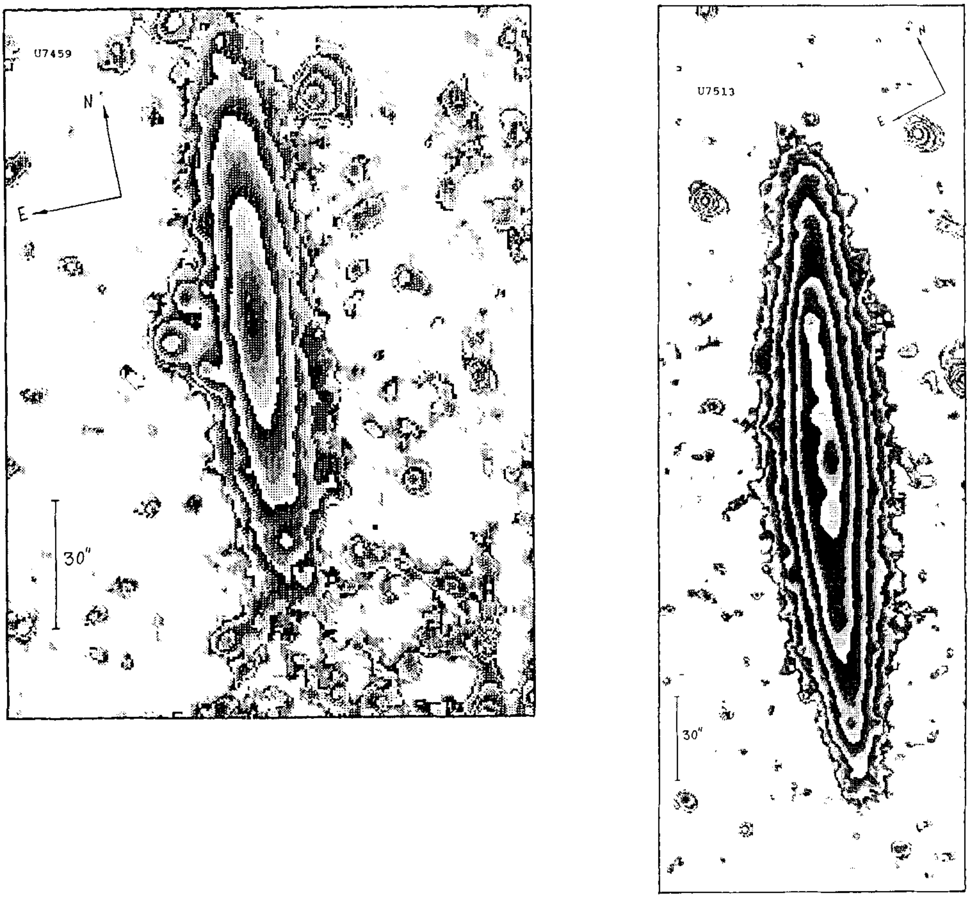

Figure 2 (*Continued*)

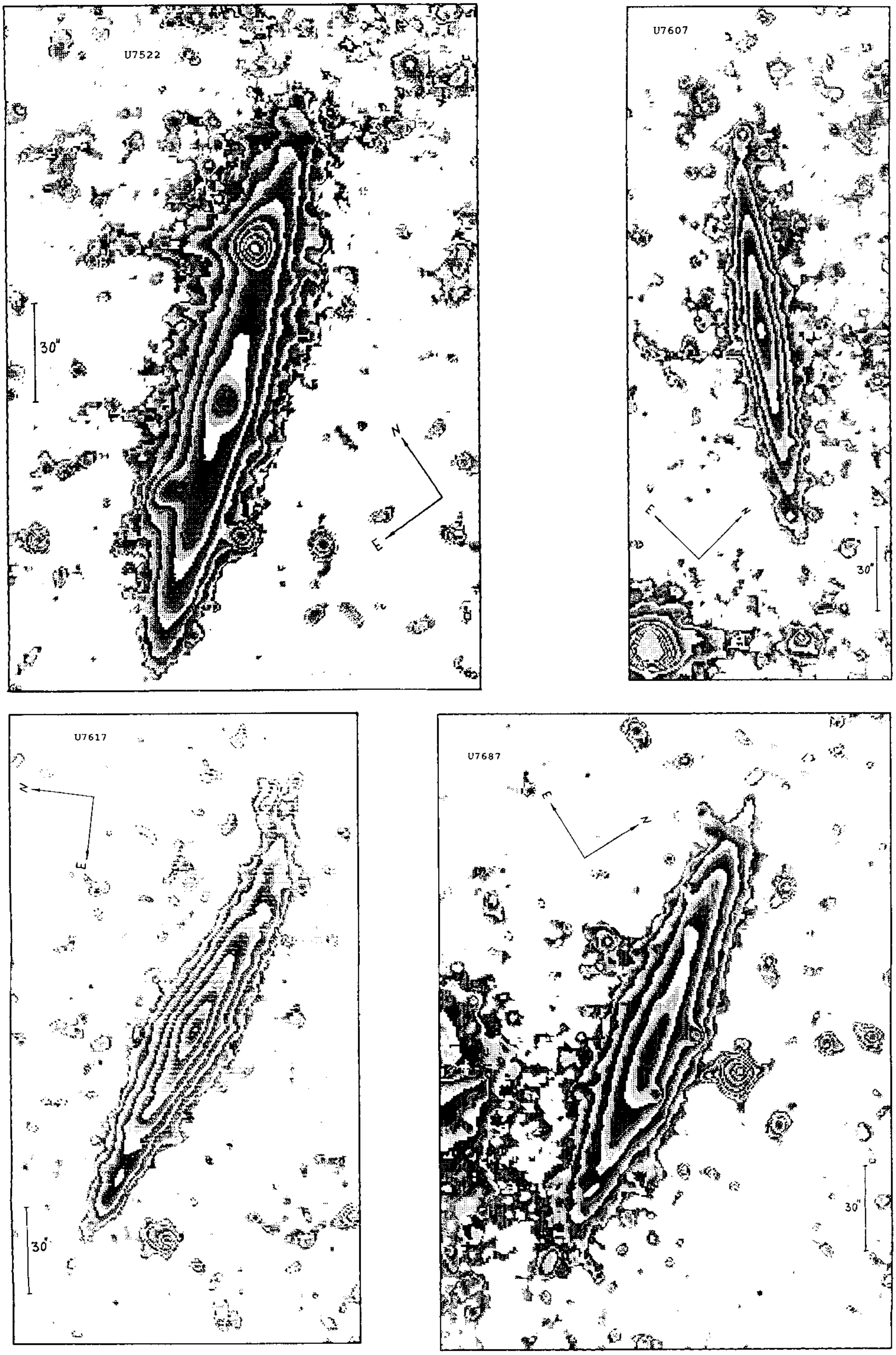

Figure 2 (*Continued*)

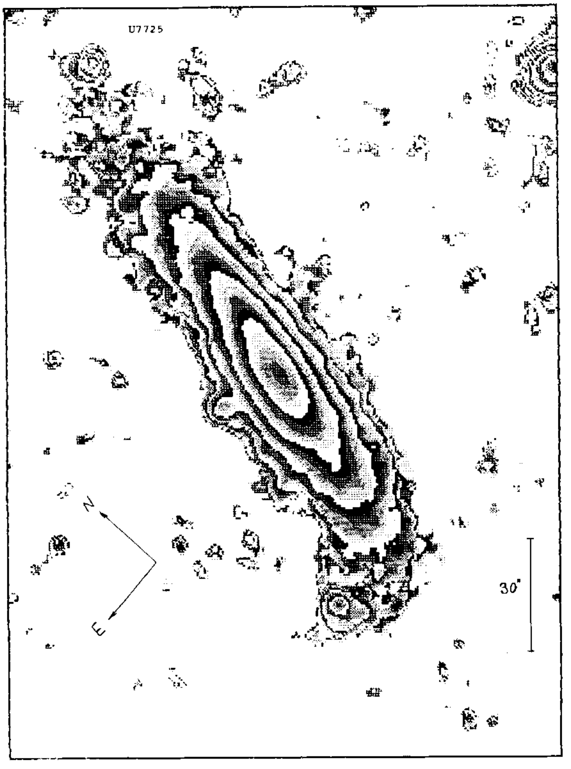

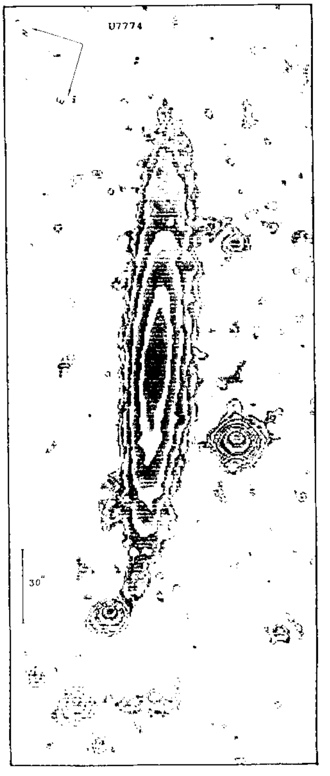

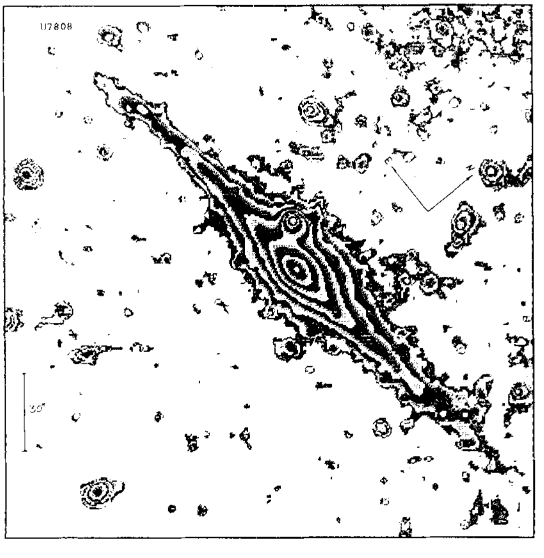

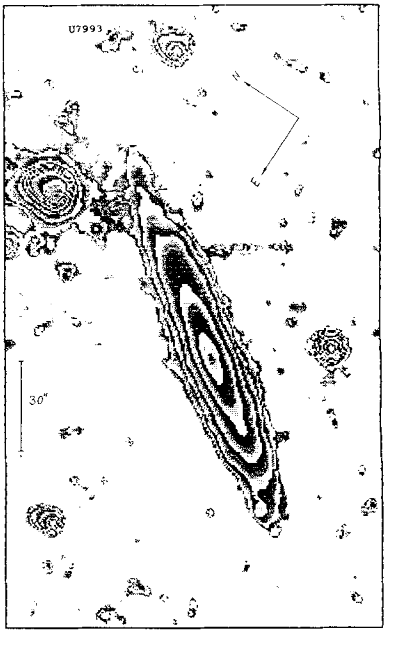

Figure 2 (*Continued*)

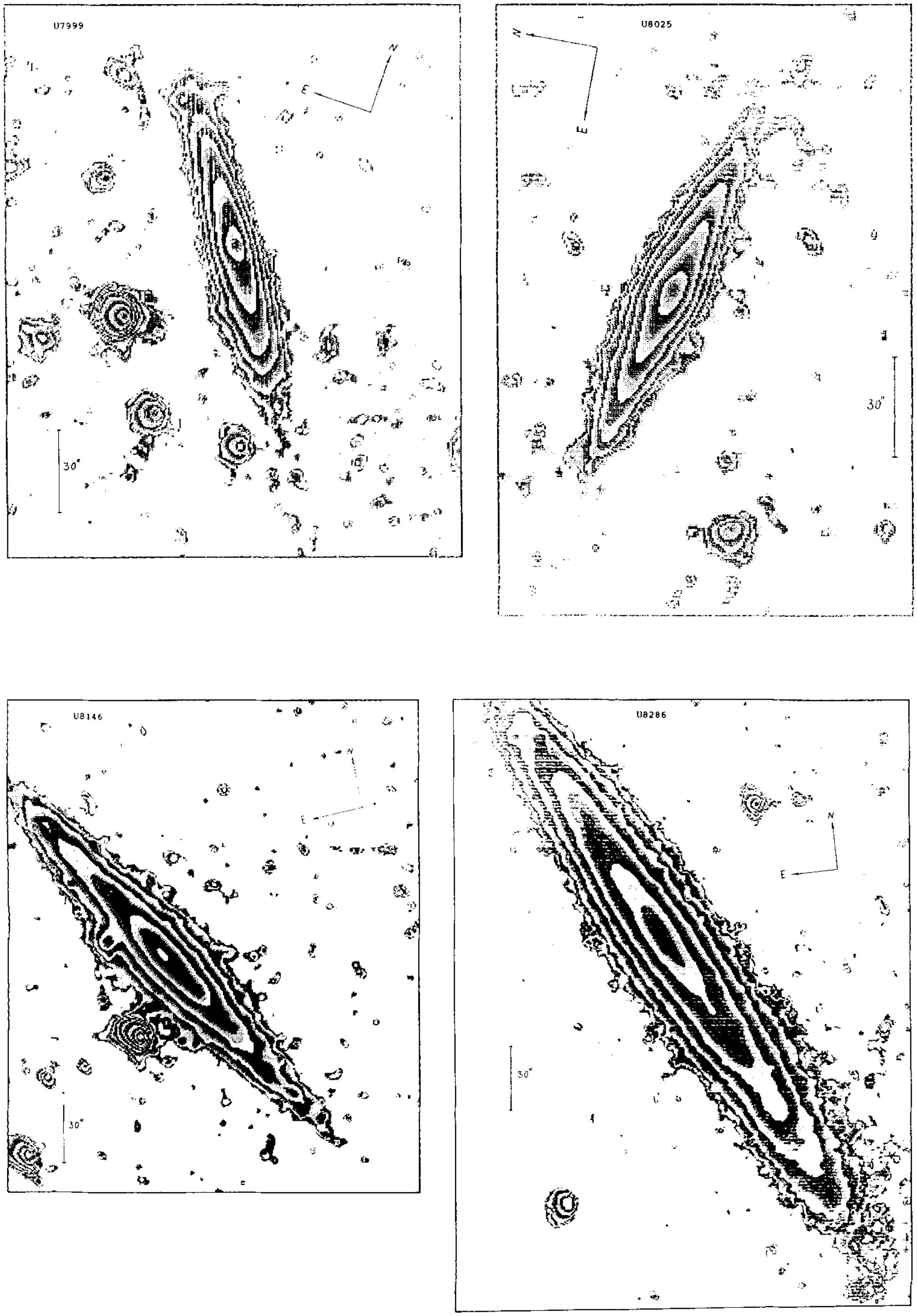

Figure 2 (*Continued*)

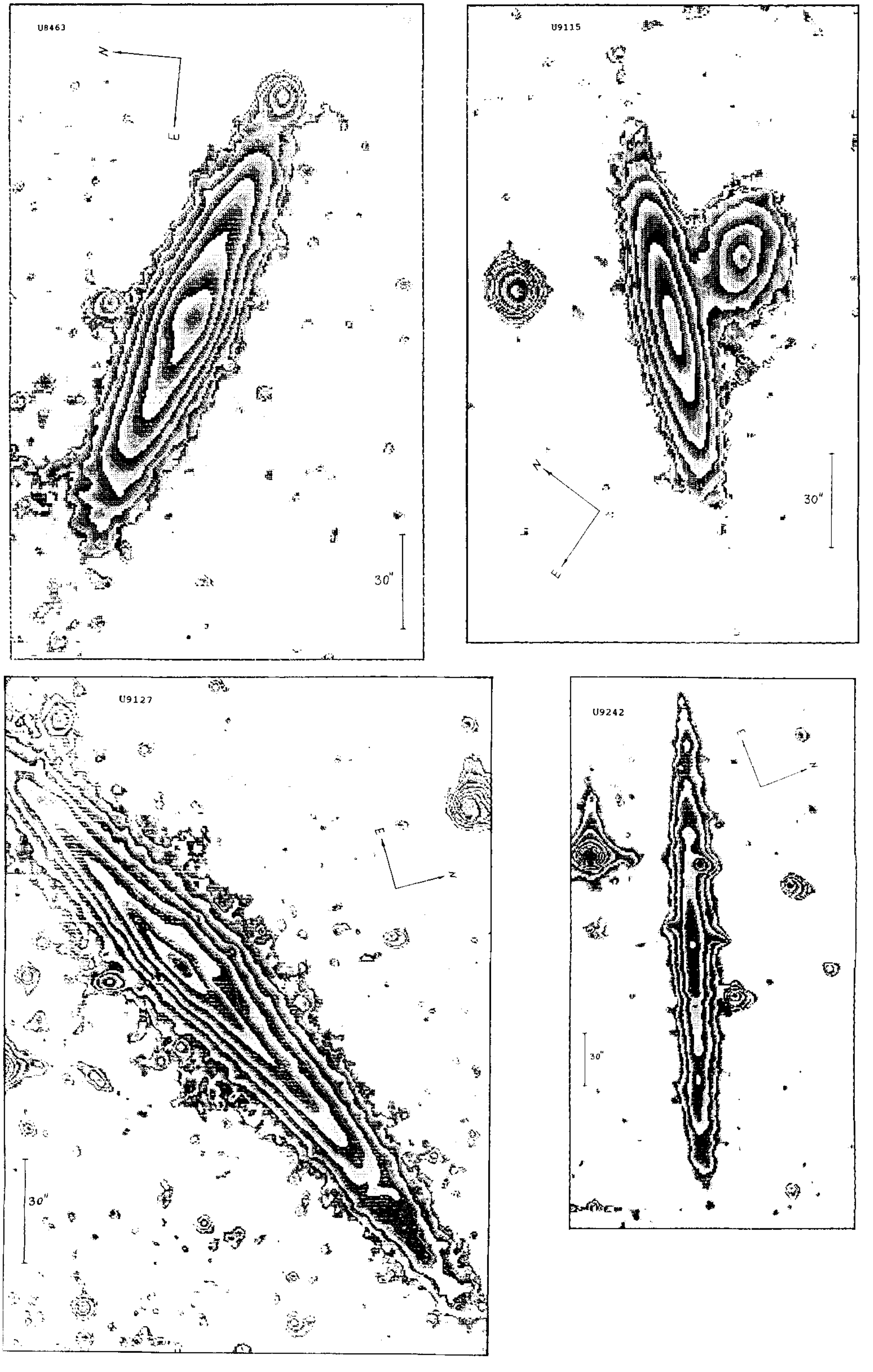

Figure 2 (*Continued*)

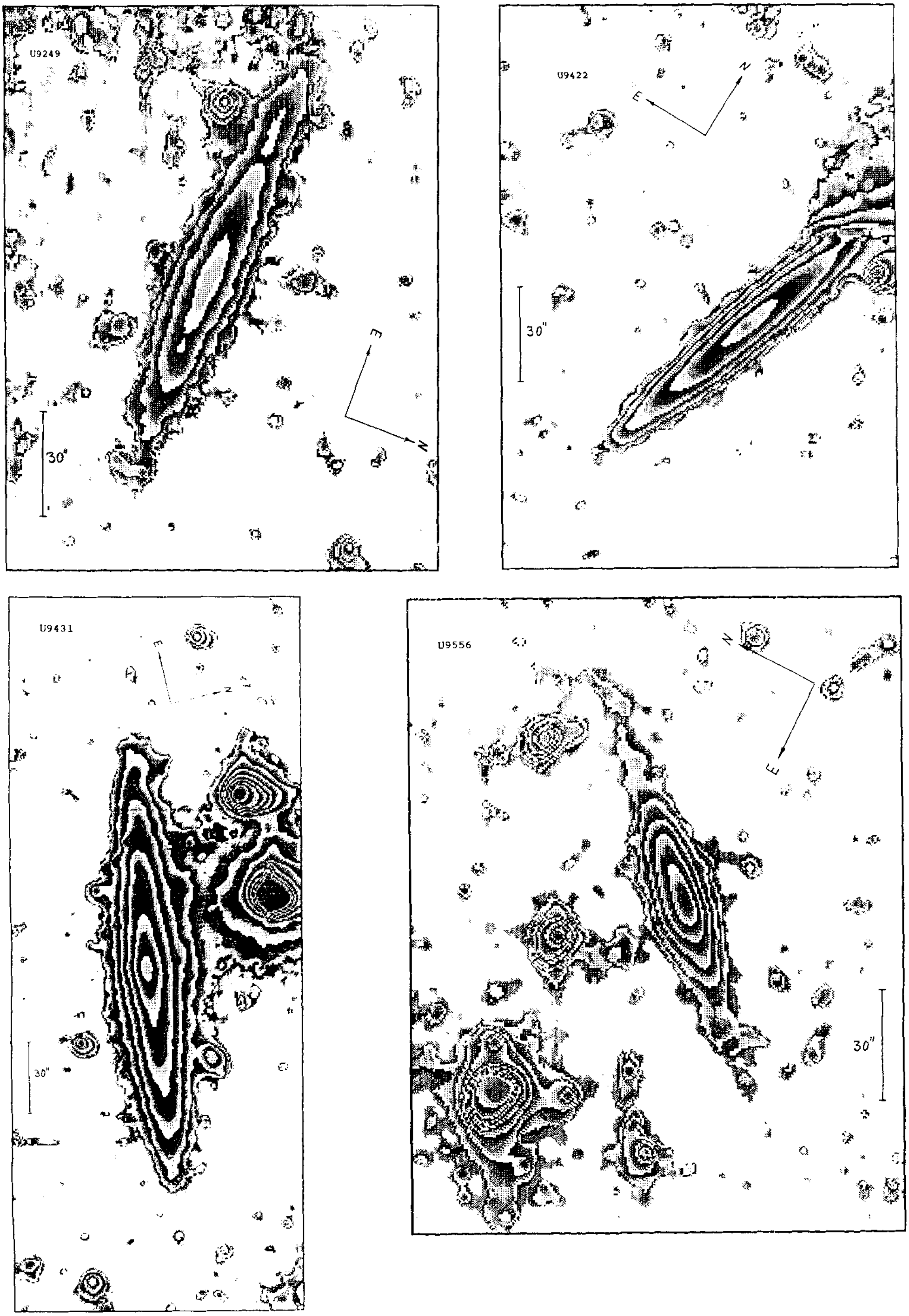

Figure 2 (*Continued*)

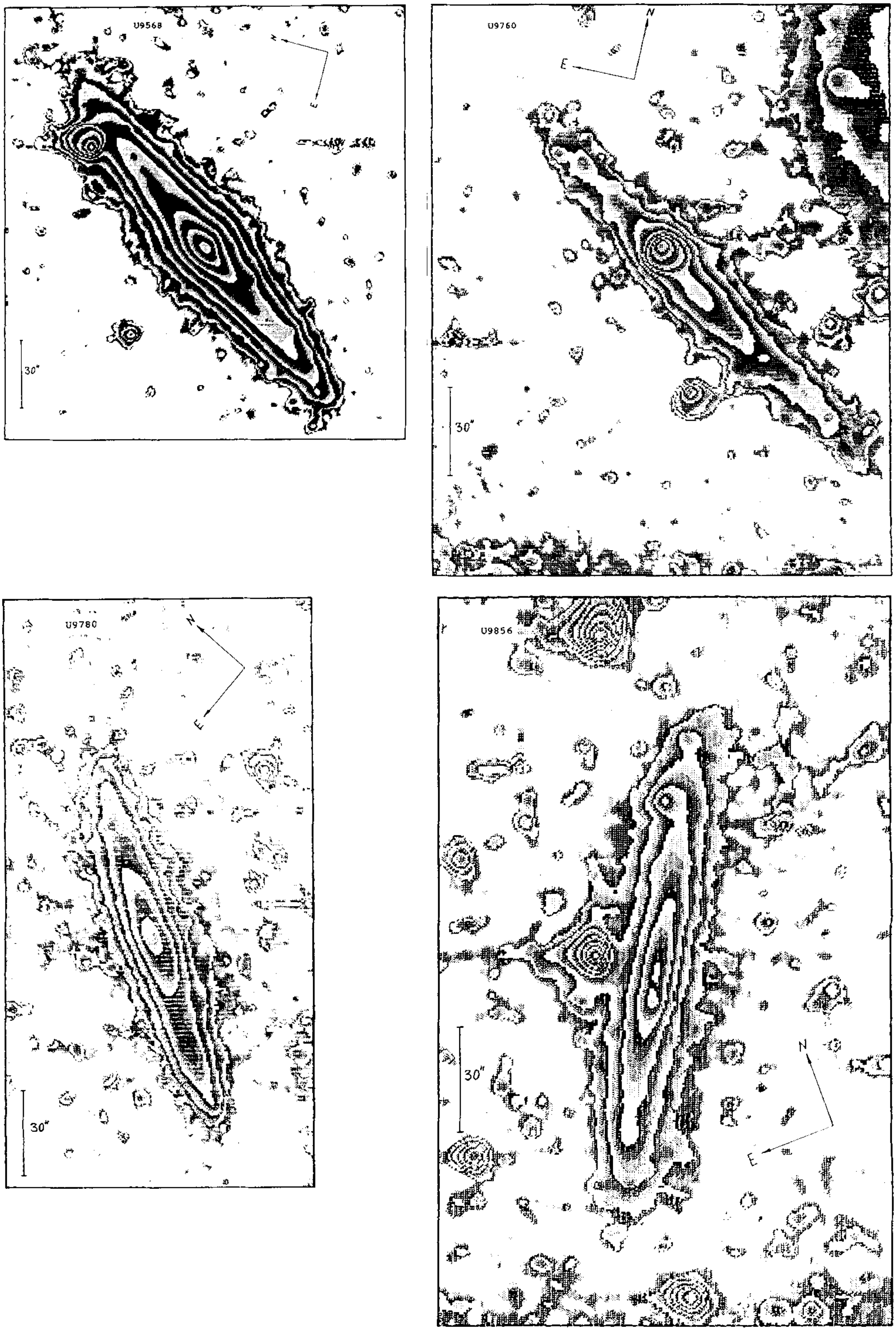

Figure 2 (*Continued*)

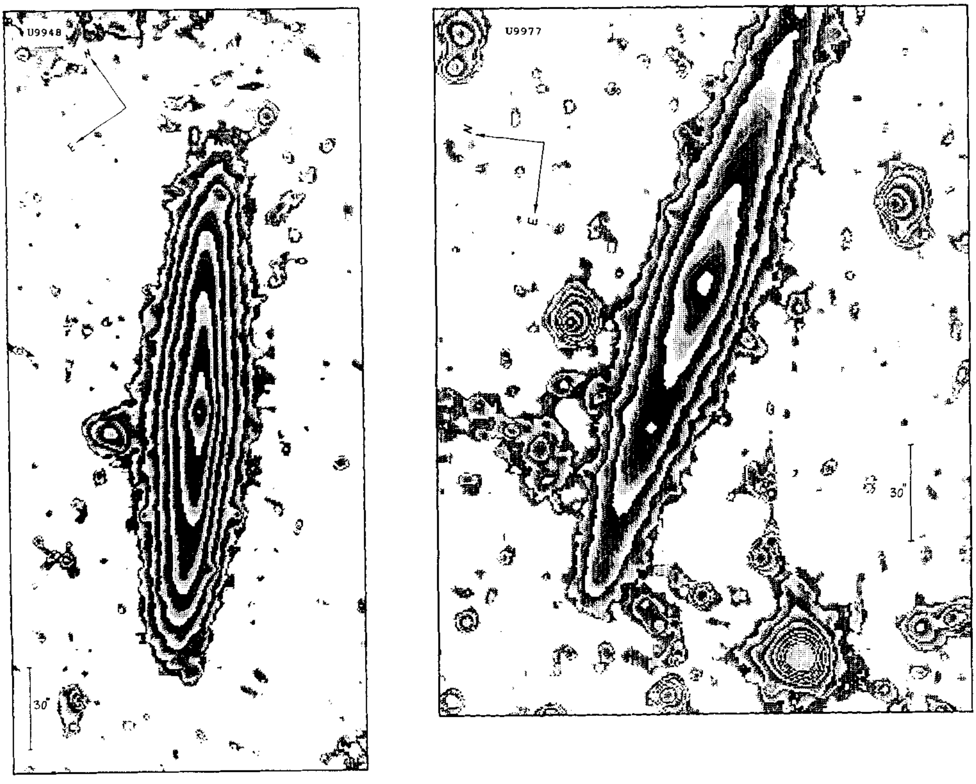

Figure 2 (*Continued*)

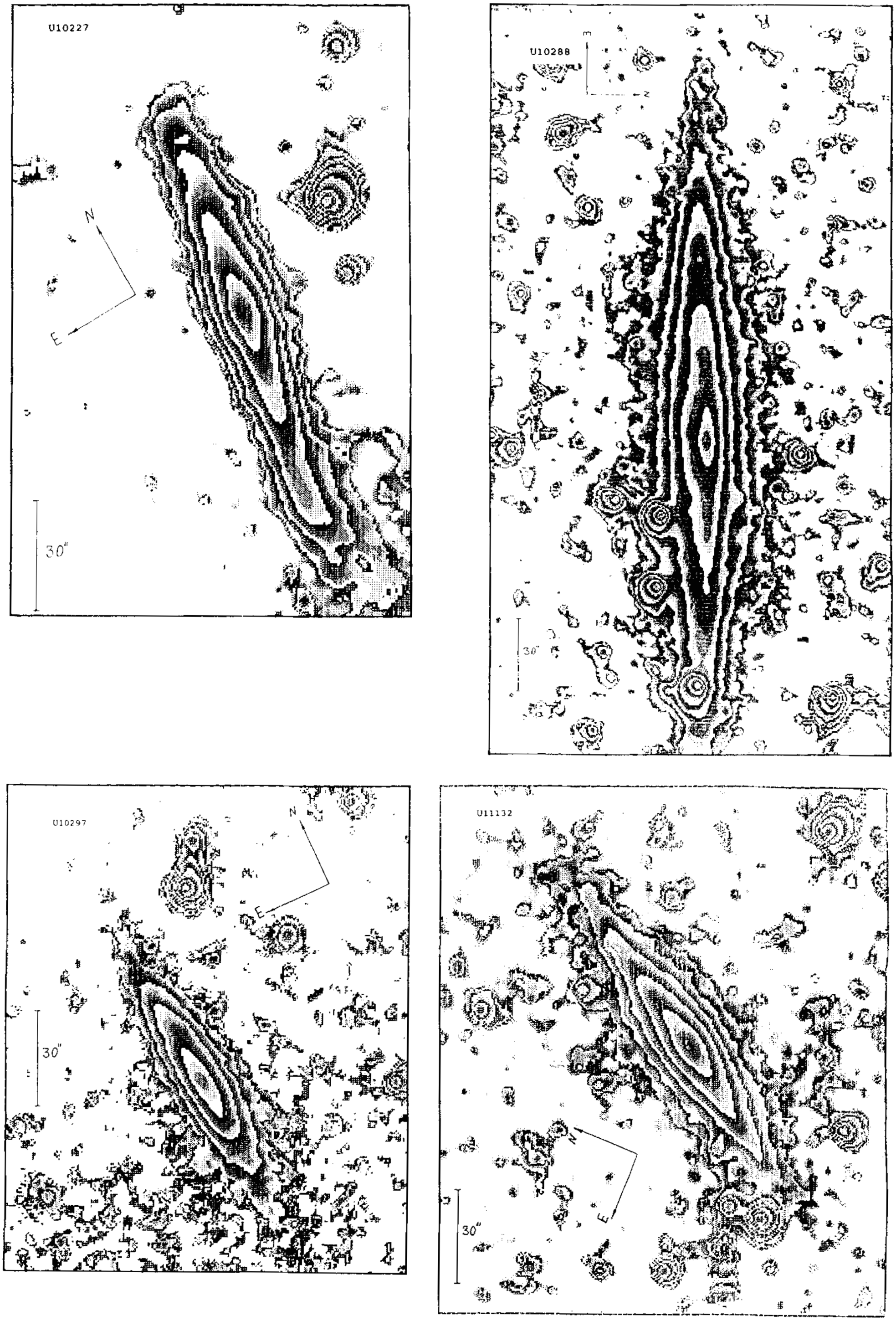

Figure 2 (*Continued*)

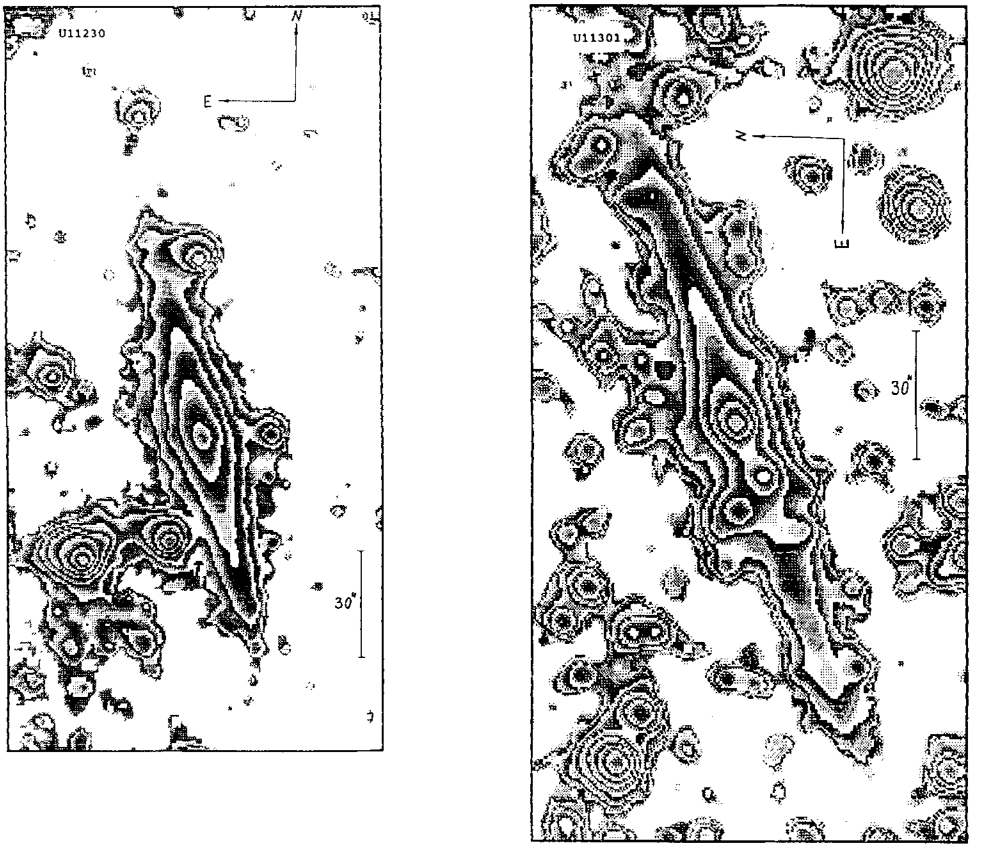

Figure 2 (*Continued*)

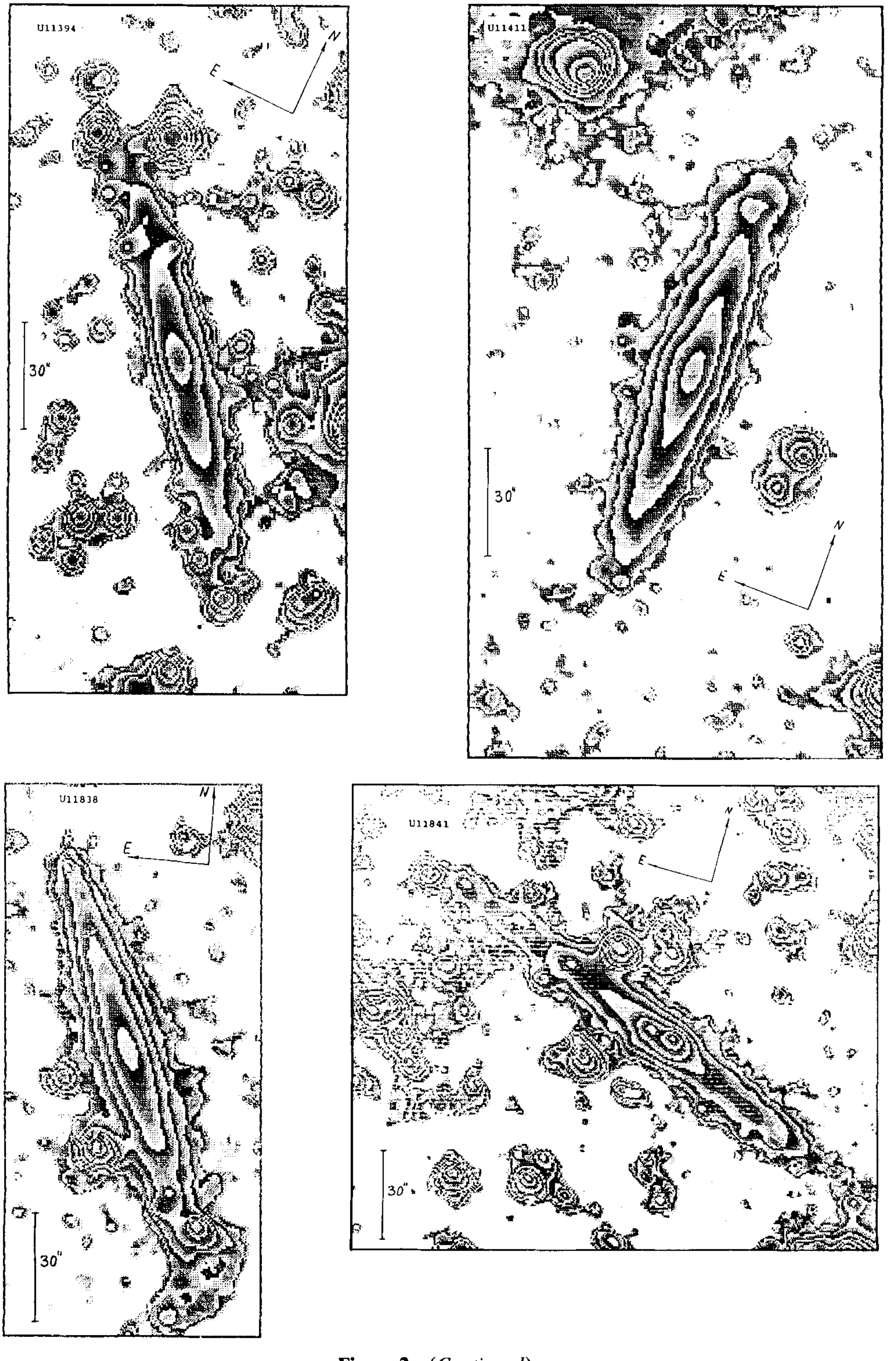

Figure 2 (*Continued*)

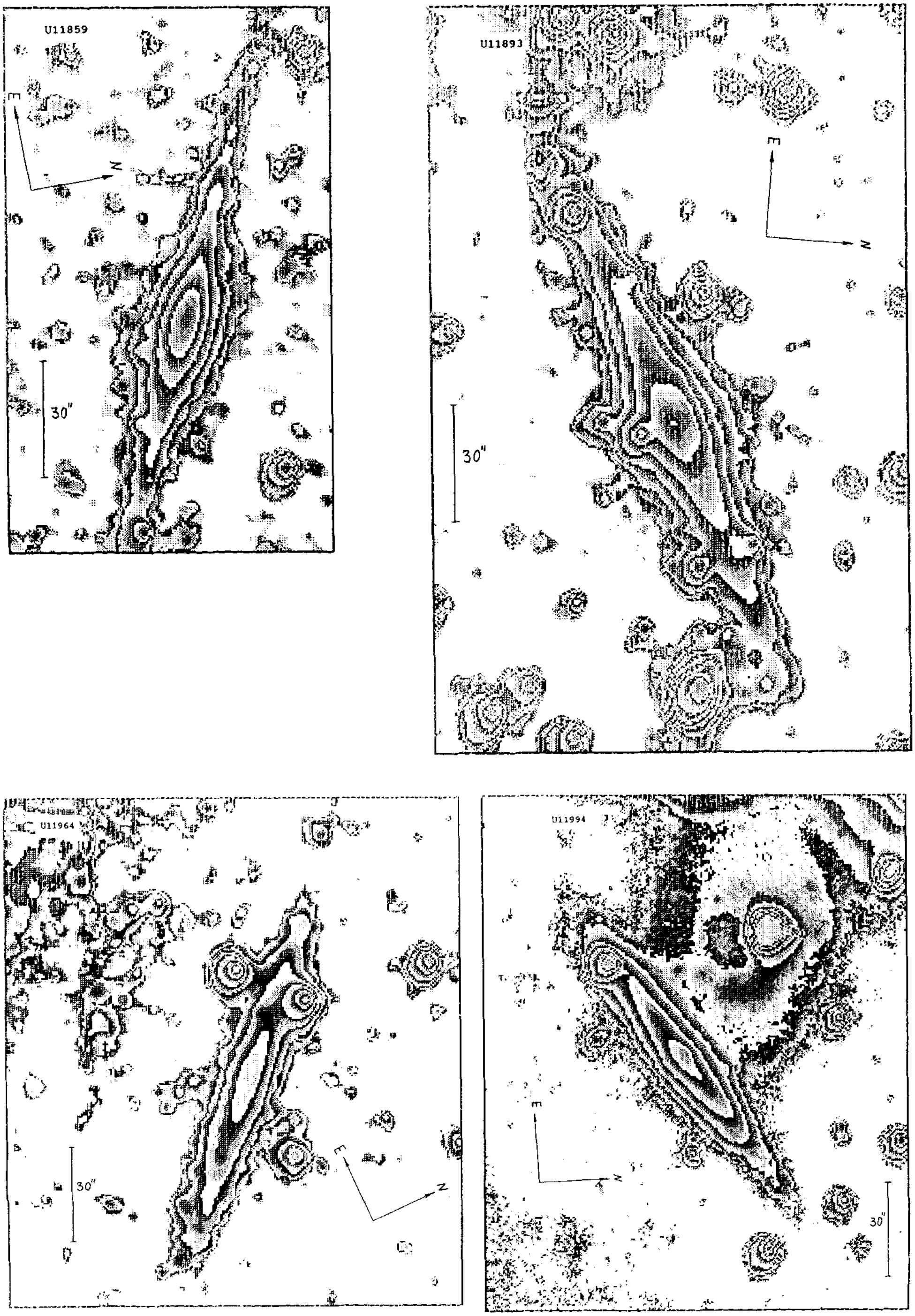

Figure 2 (*Continued*)

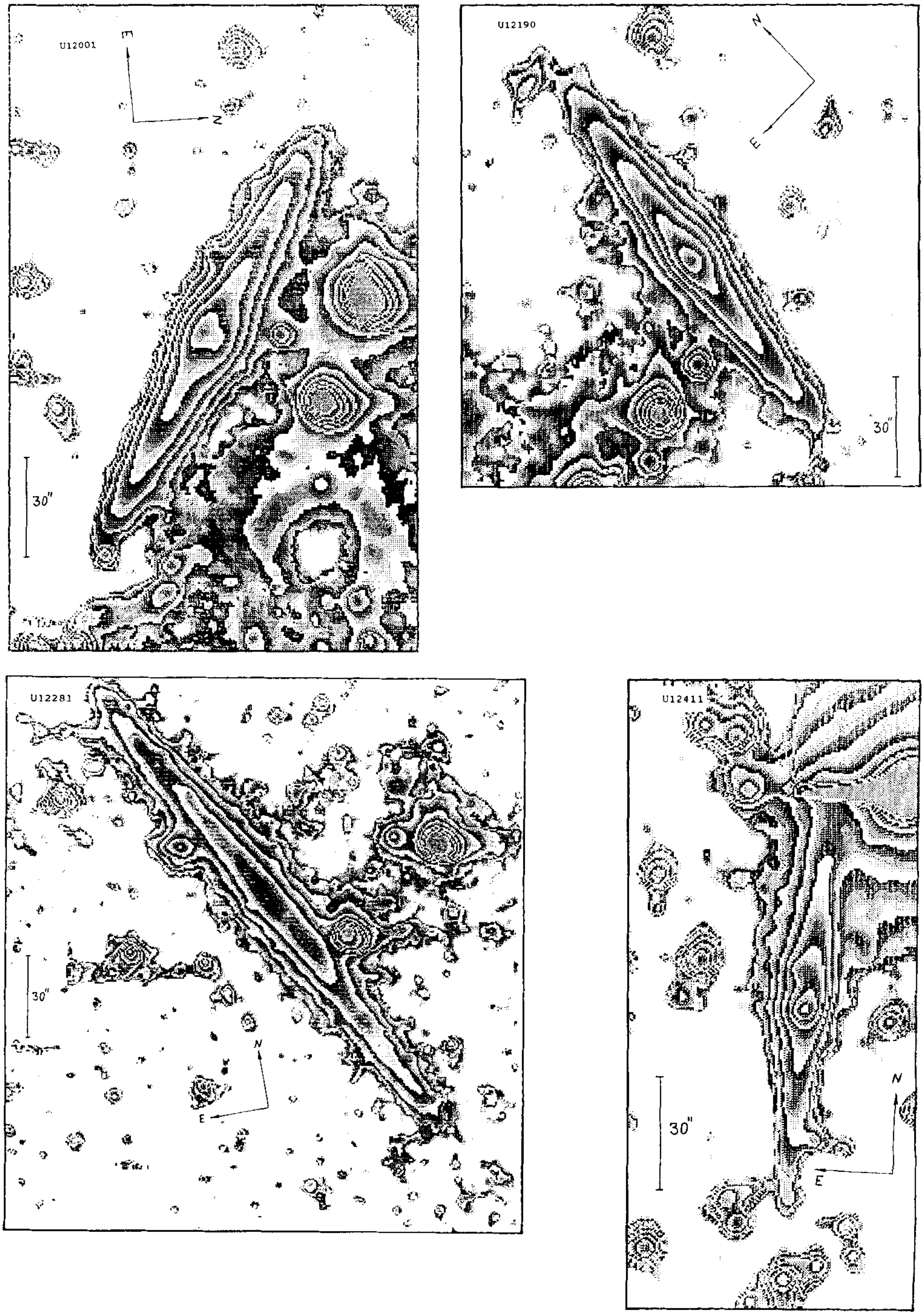

Figure 2 (*Continued*)

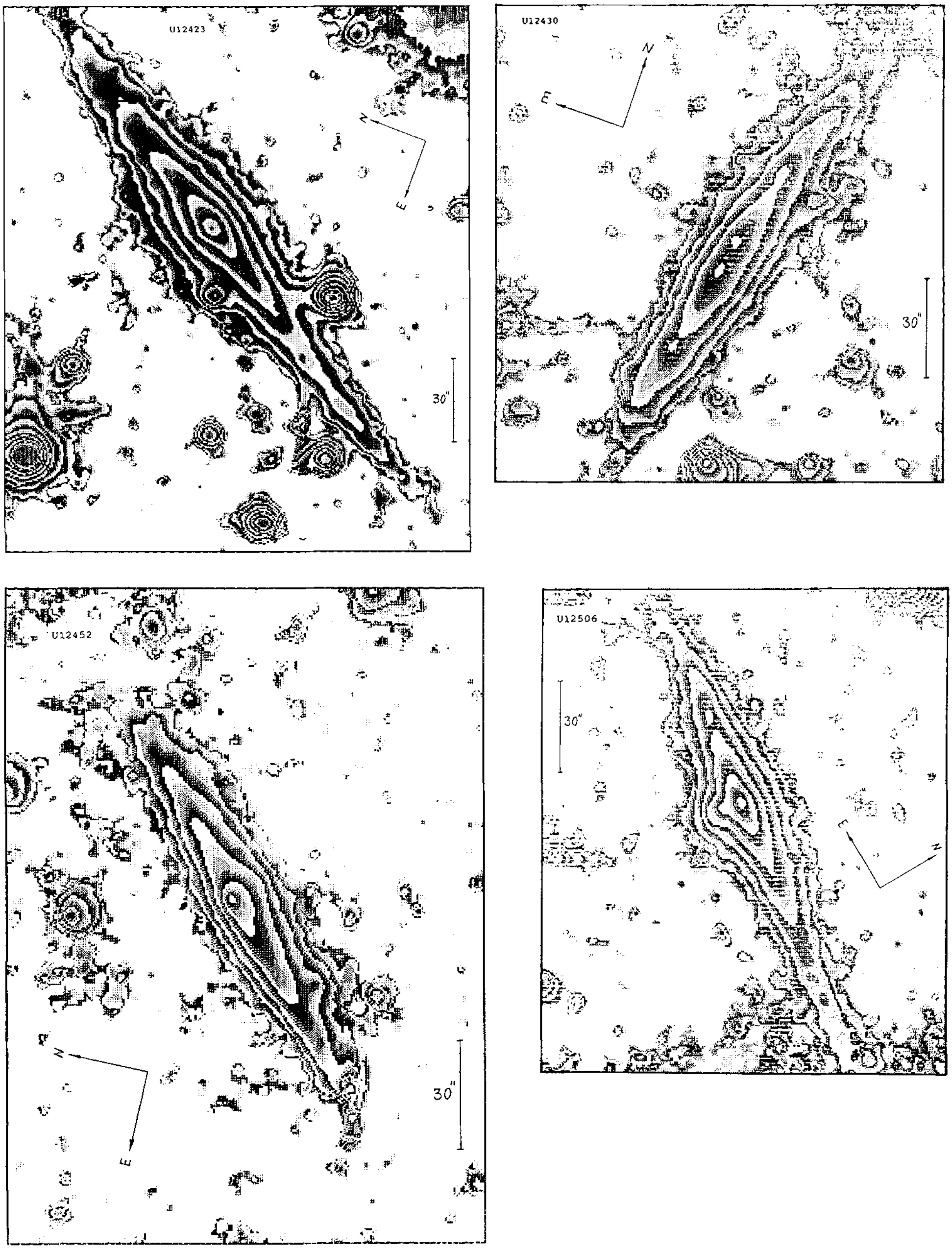

Figure 2 (*Continued*)

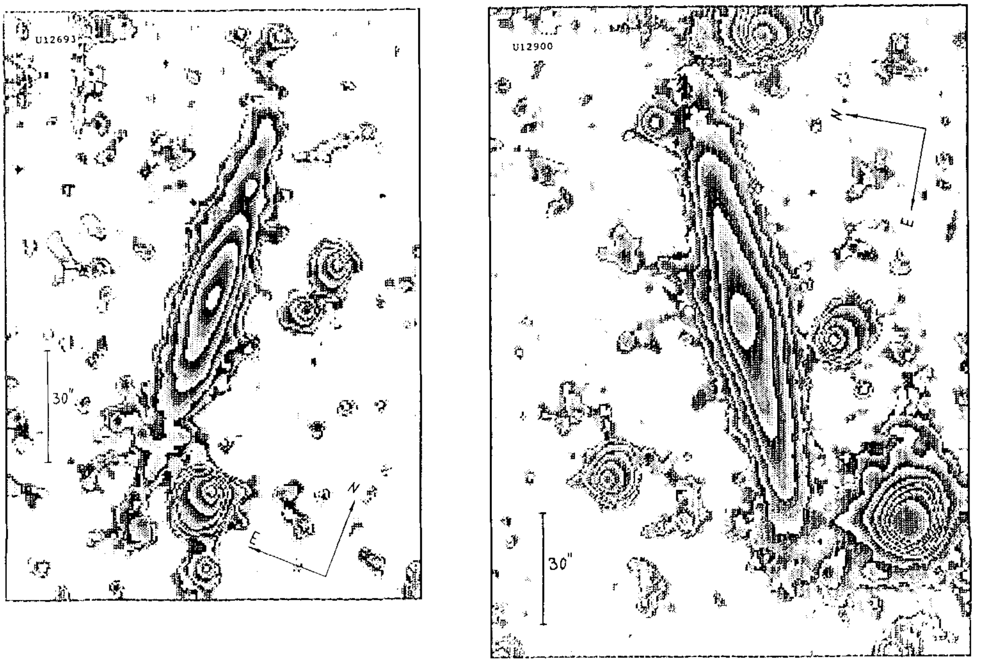

Figure 2 (*Continued*)

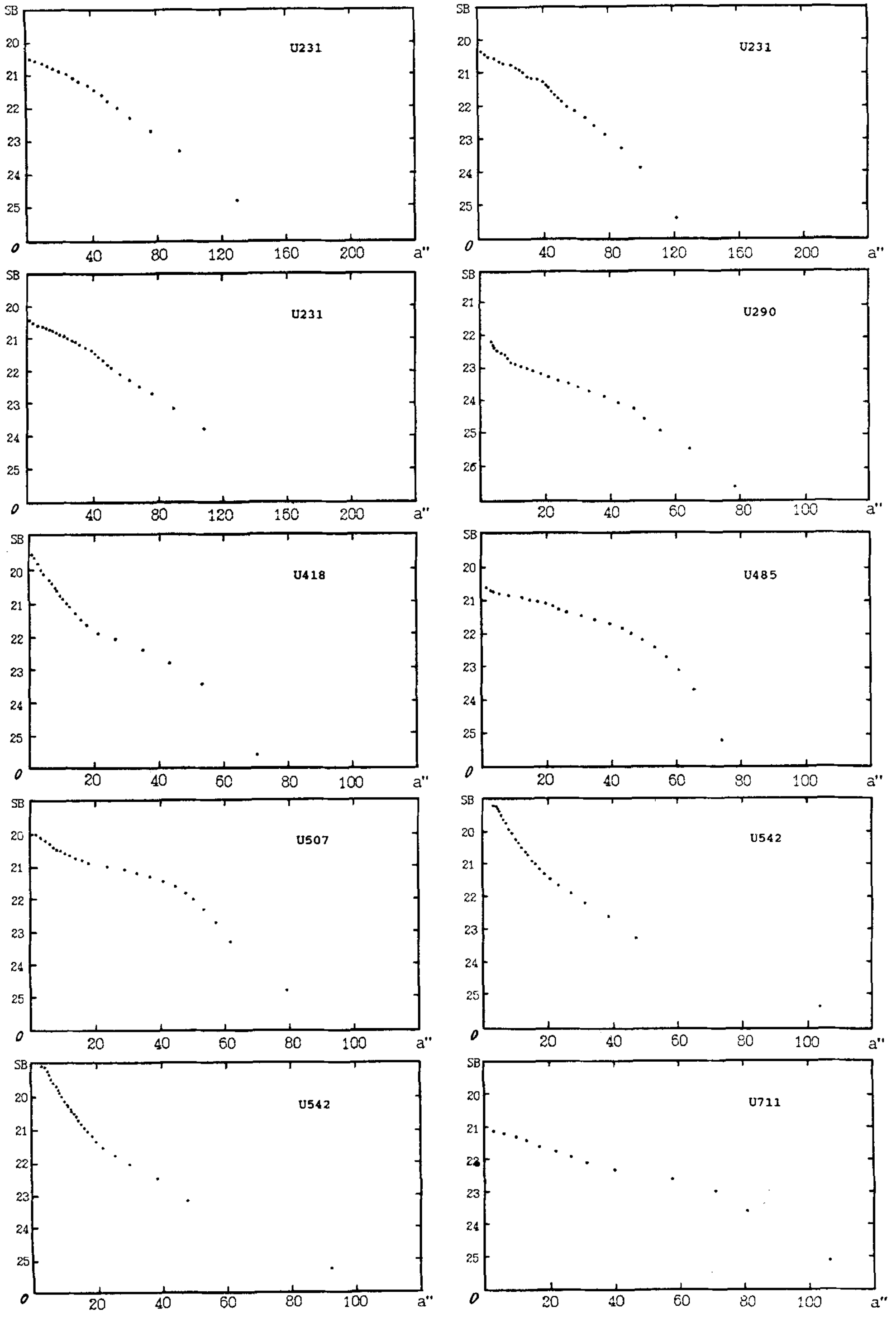

Figure 3 Distribution of the red surface brightness (in mag/arc second^2) along the major axis (in arc seconds) for 120 flat galaxies. In some cases (UGC 231, 542, etc.) the luminosity profiles were obtained by different CCD-frames.

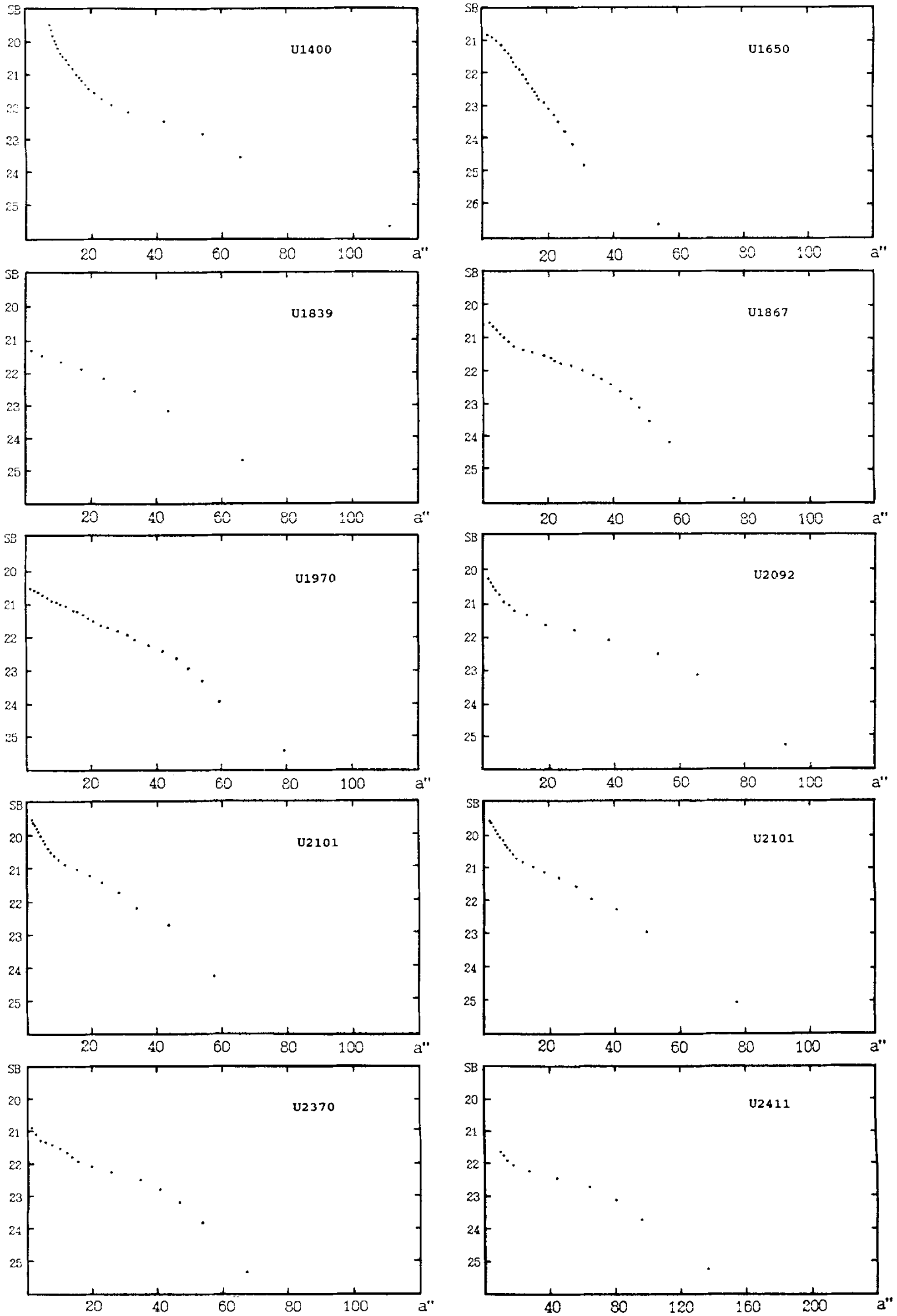

Figure 3 (*Continued*)

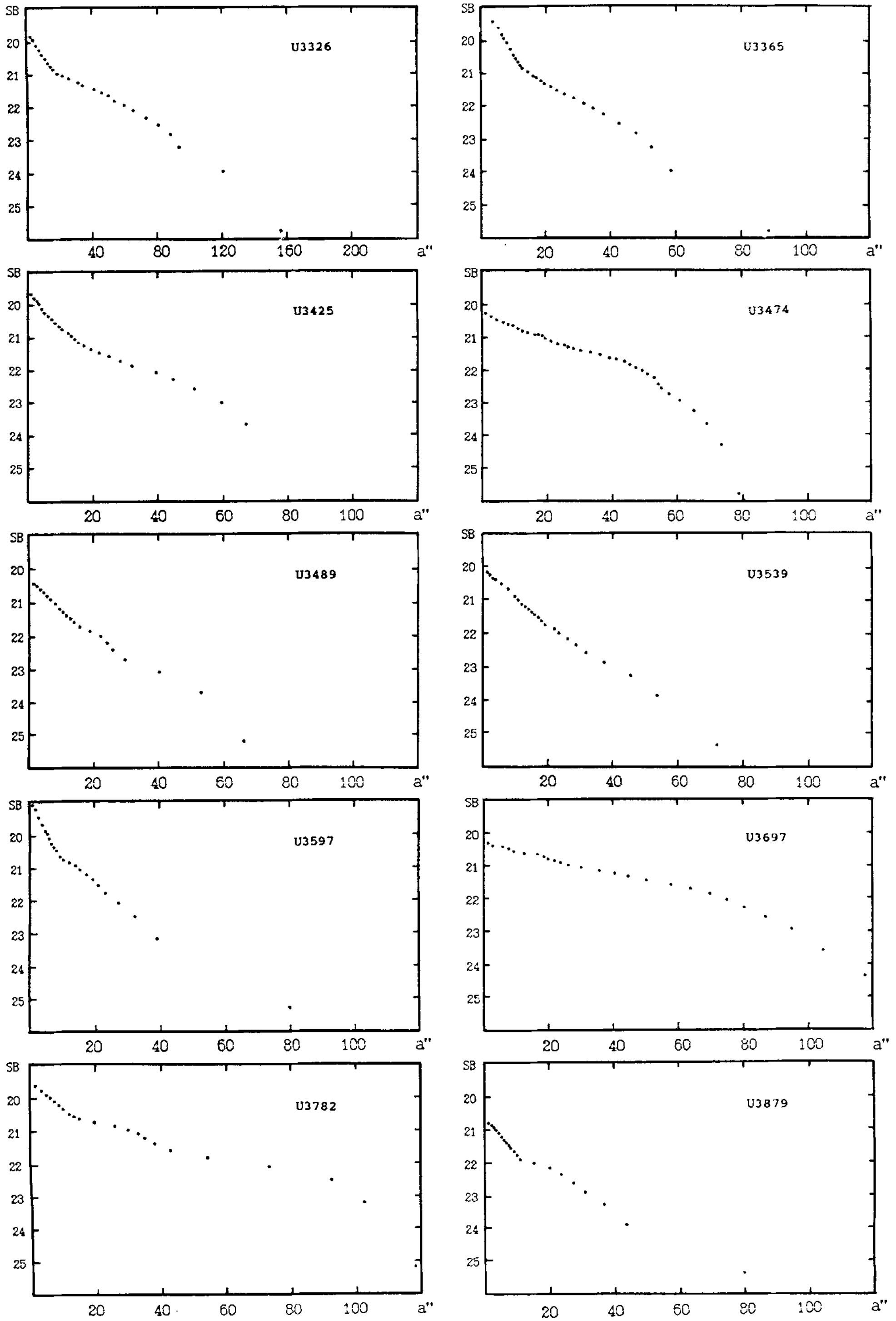

Figure 3 (*Continued*)

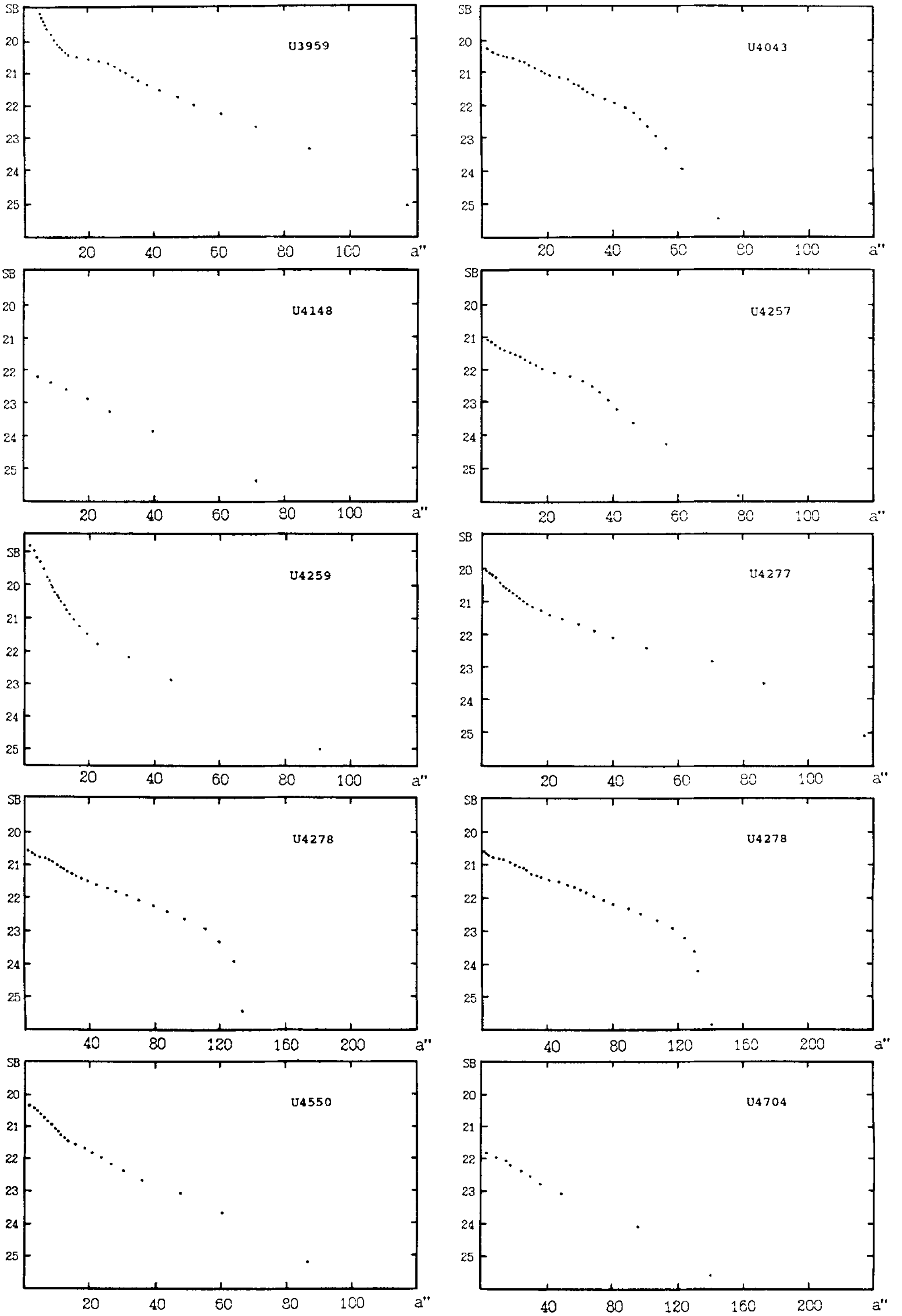

Figure 3 (*Continued*)

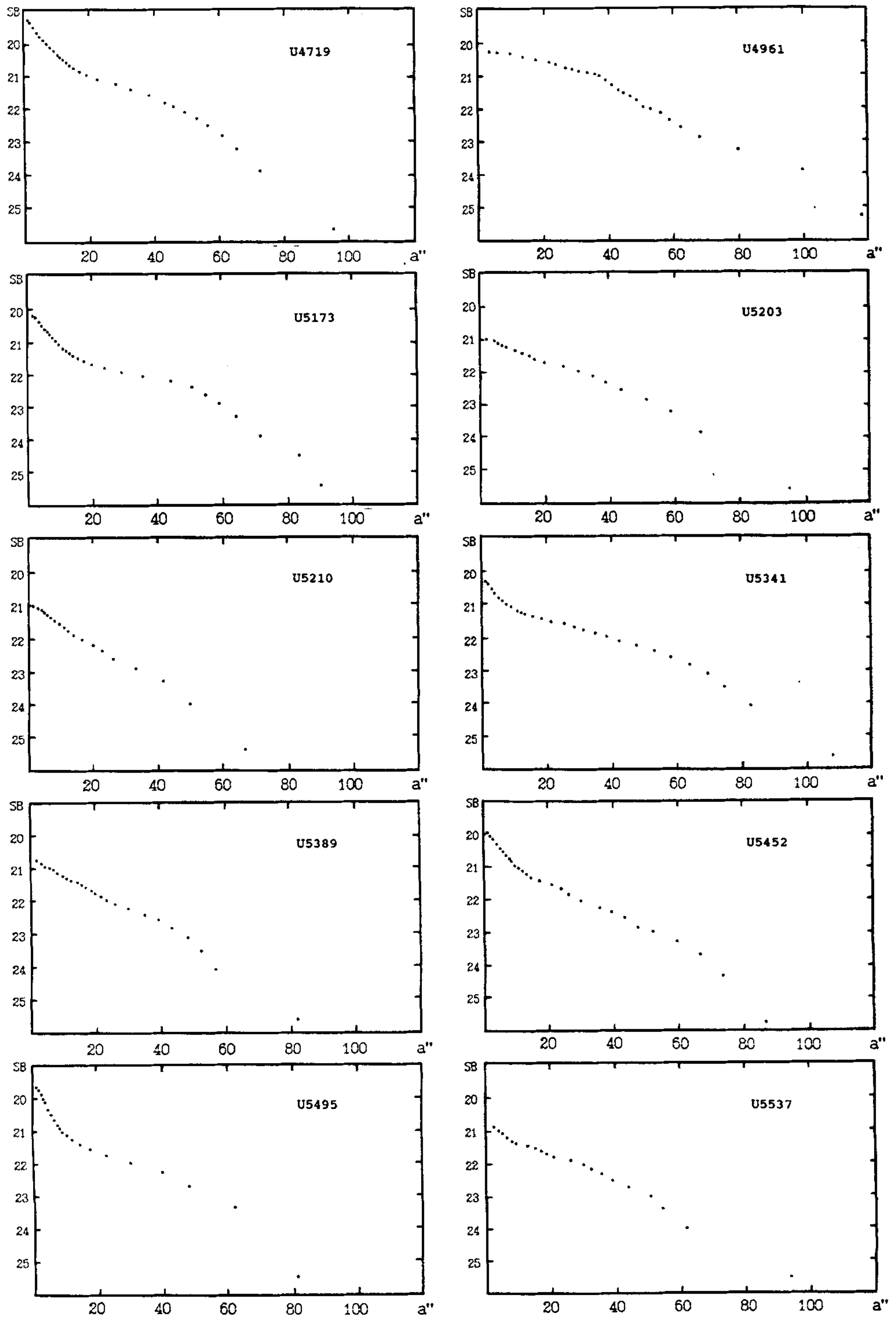

Figure 3 (*Continued*)

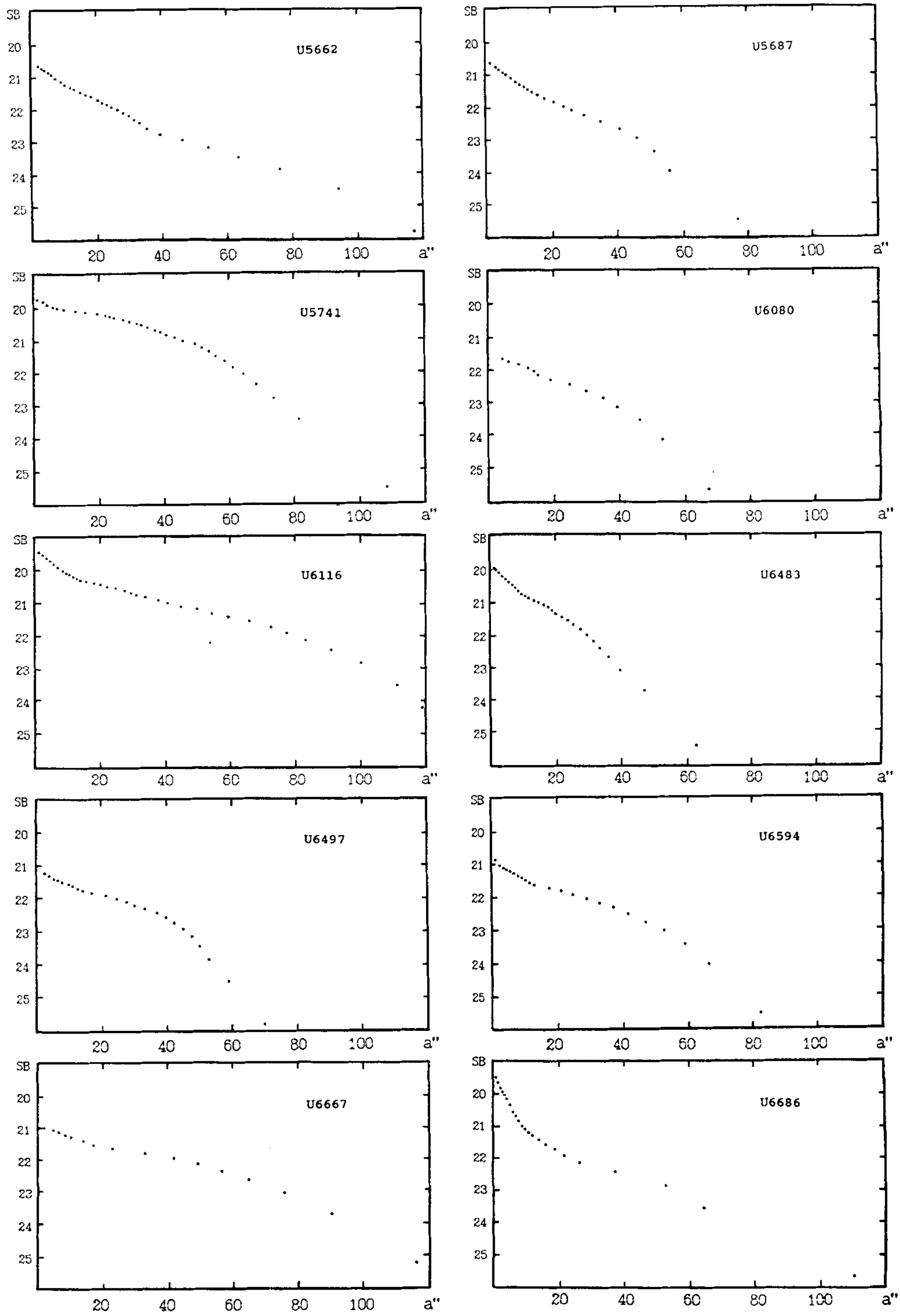

Figure 3 (*Continued*)

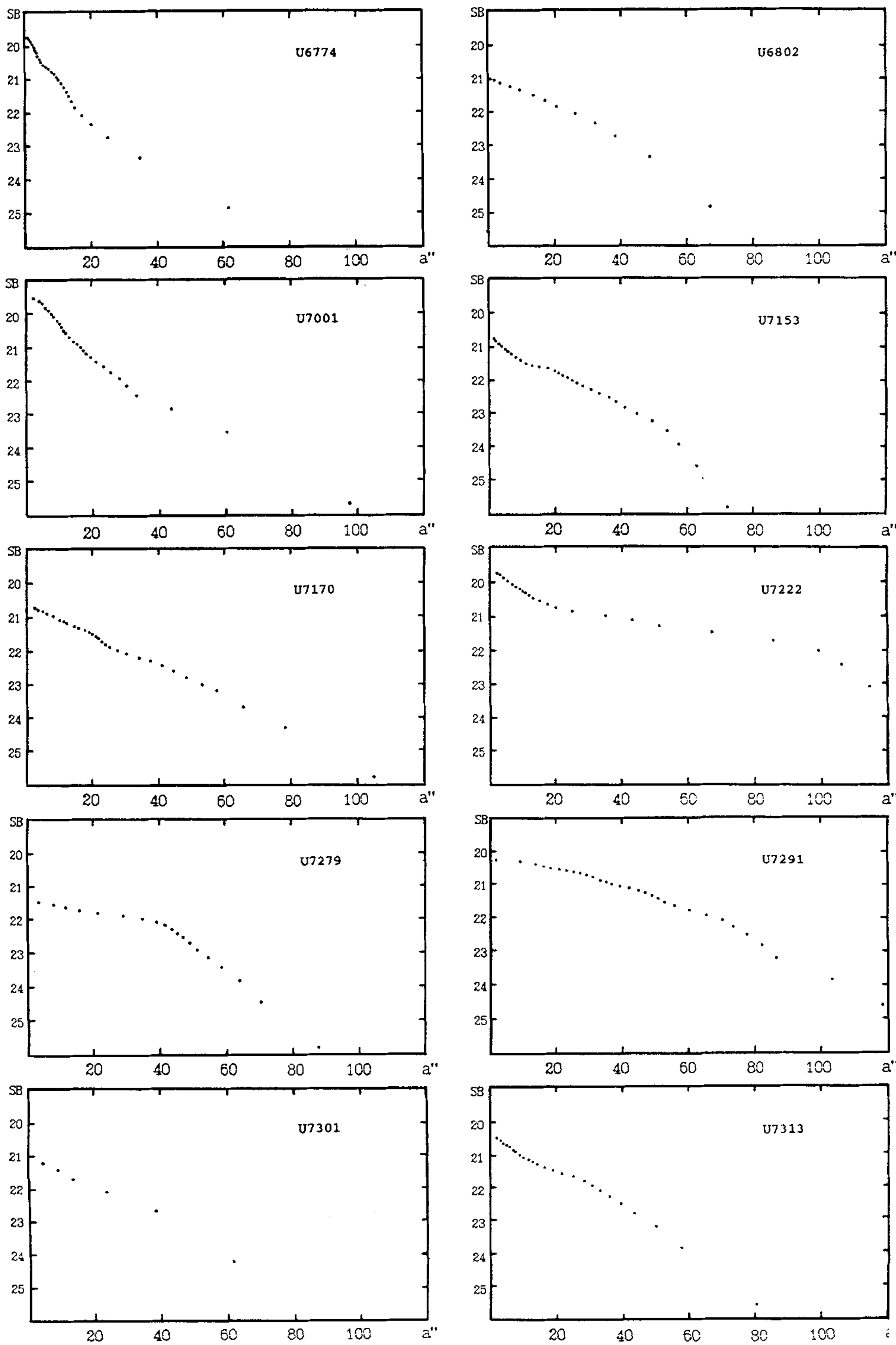

Figure 3 (*Continued*)

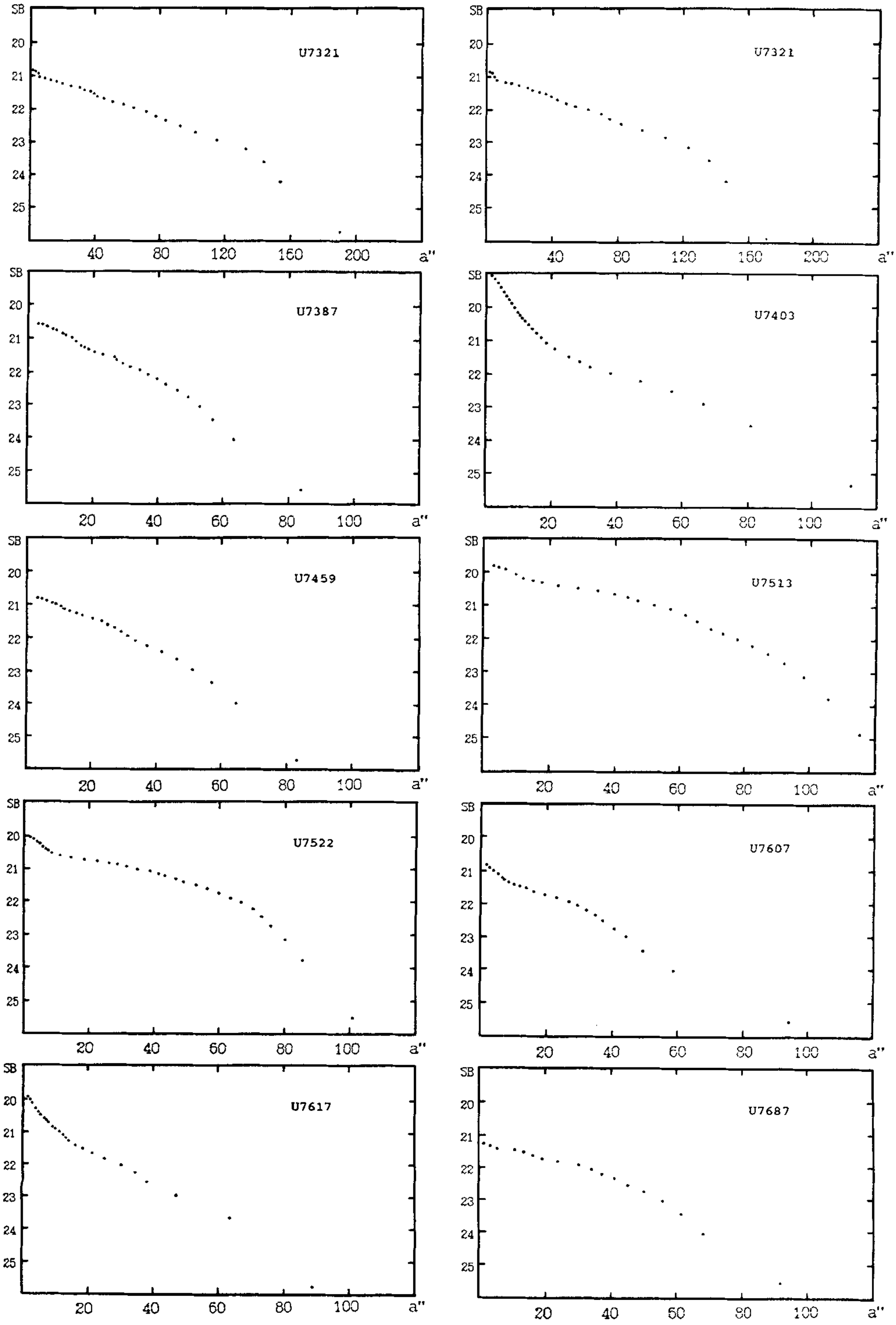

Figure 3 (*Continued*)

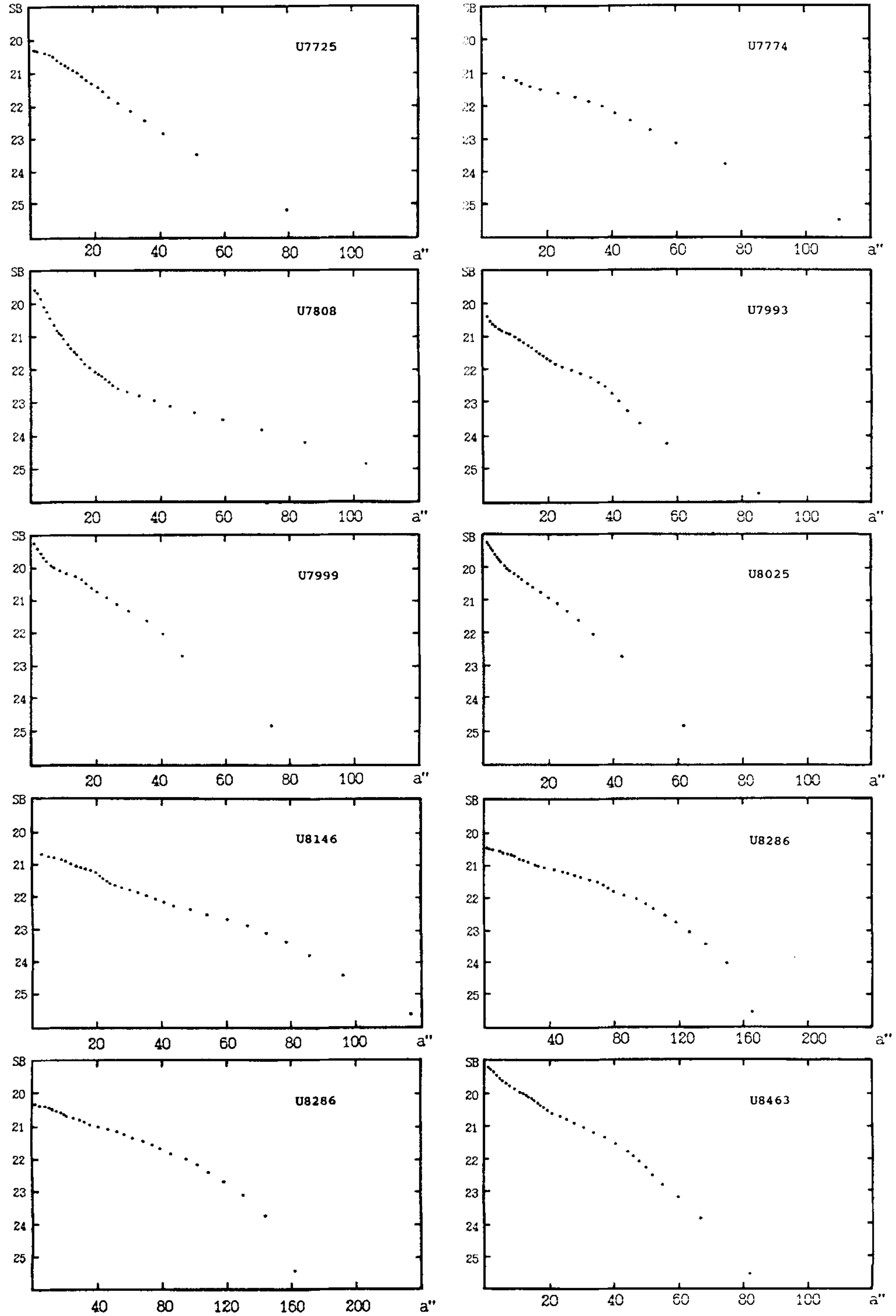

Figure 3 (*Continued*)

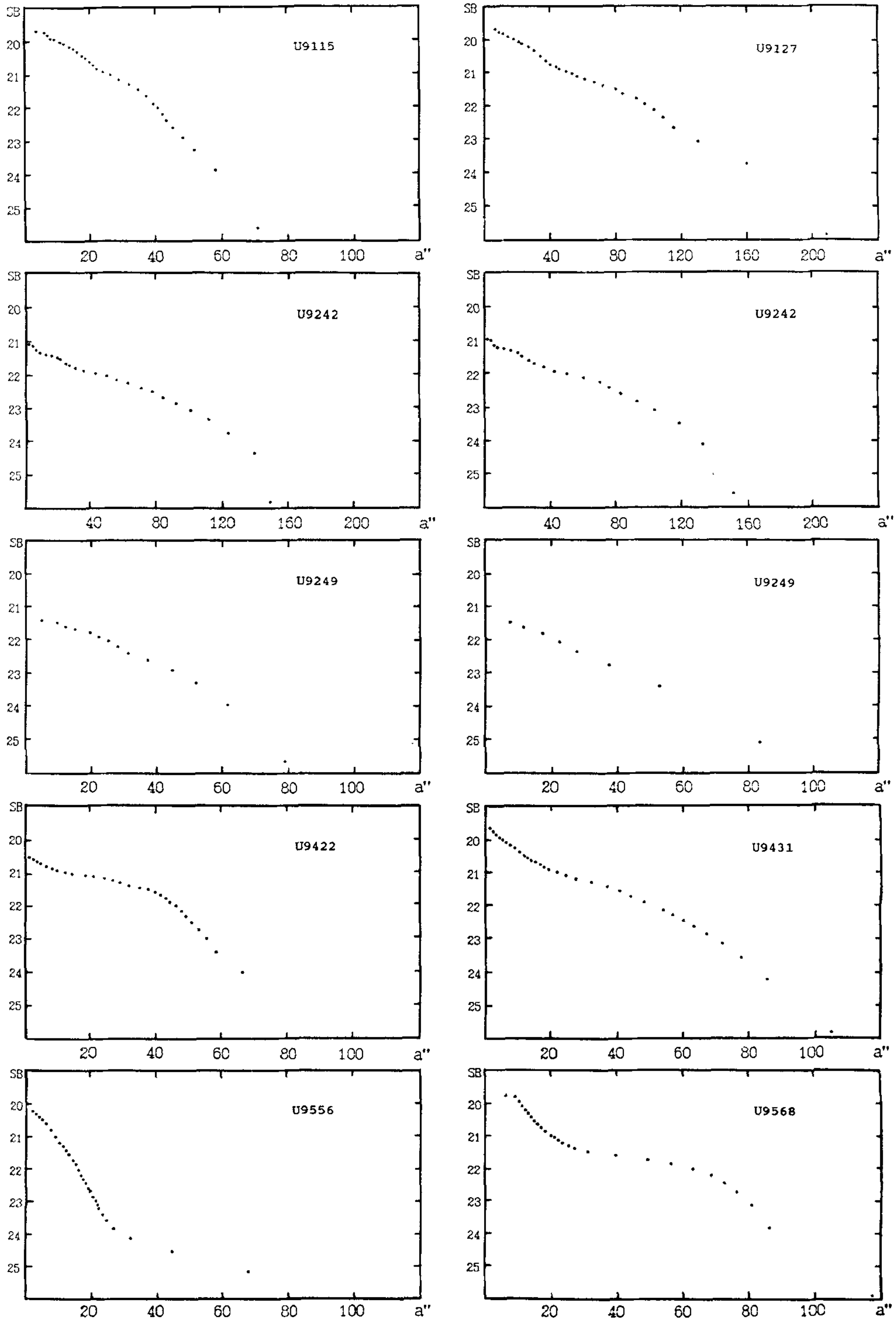

Figure 3 (*Continued*)

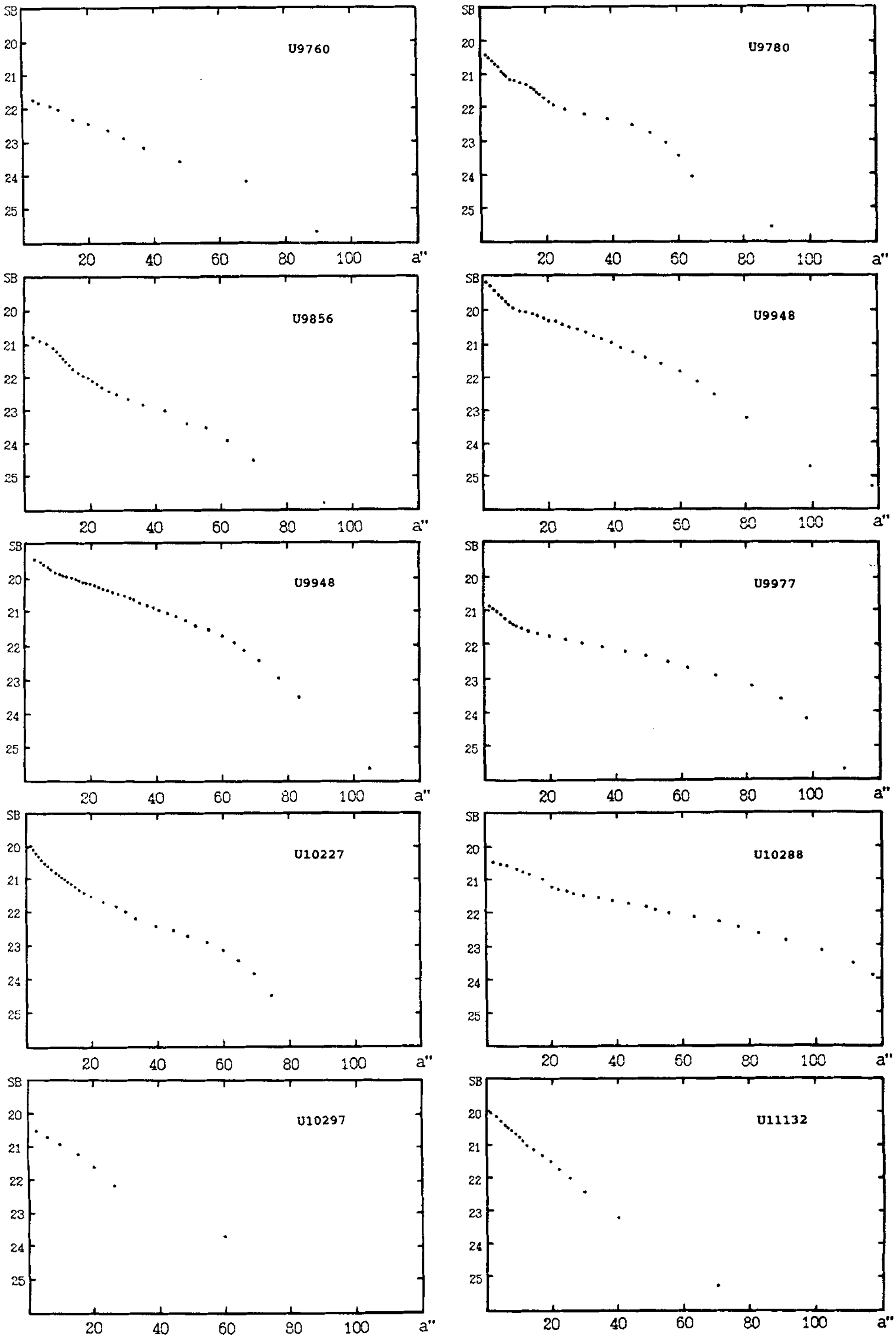

Figure 3 (*Continued*)

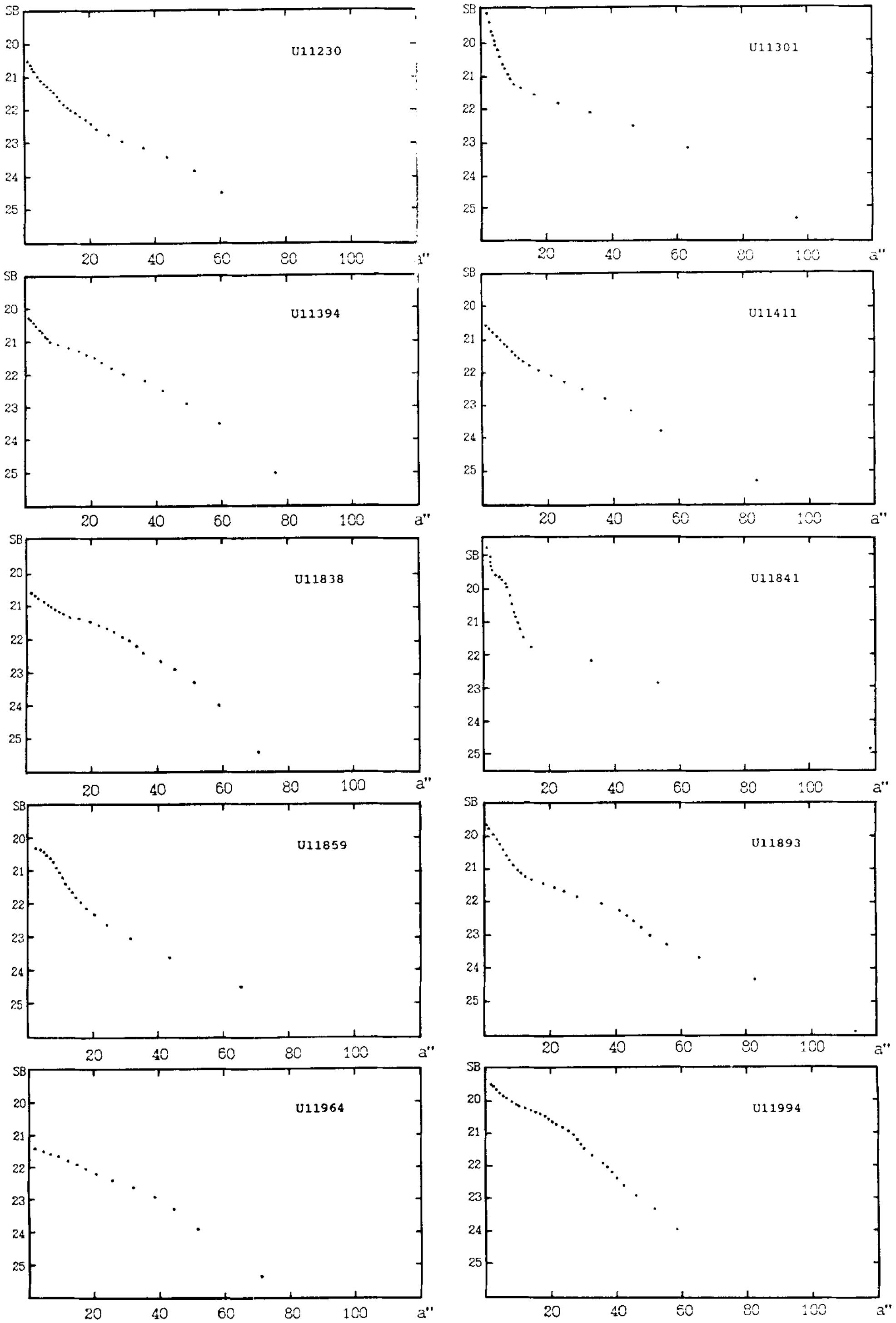

Figure 3 (*Continued*)

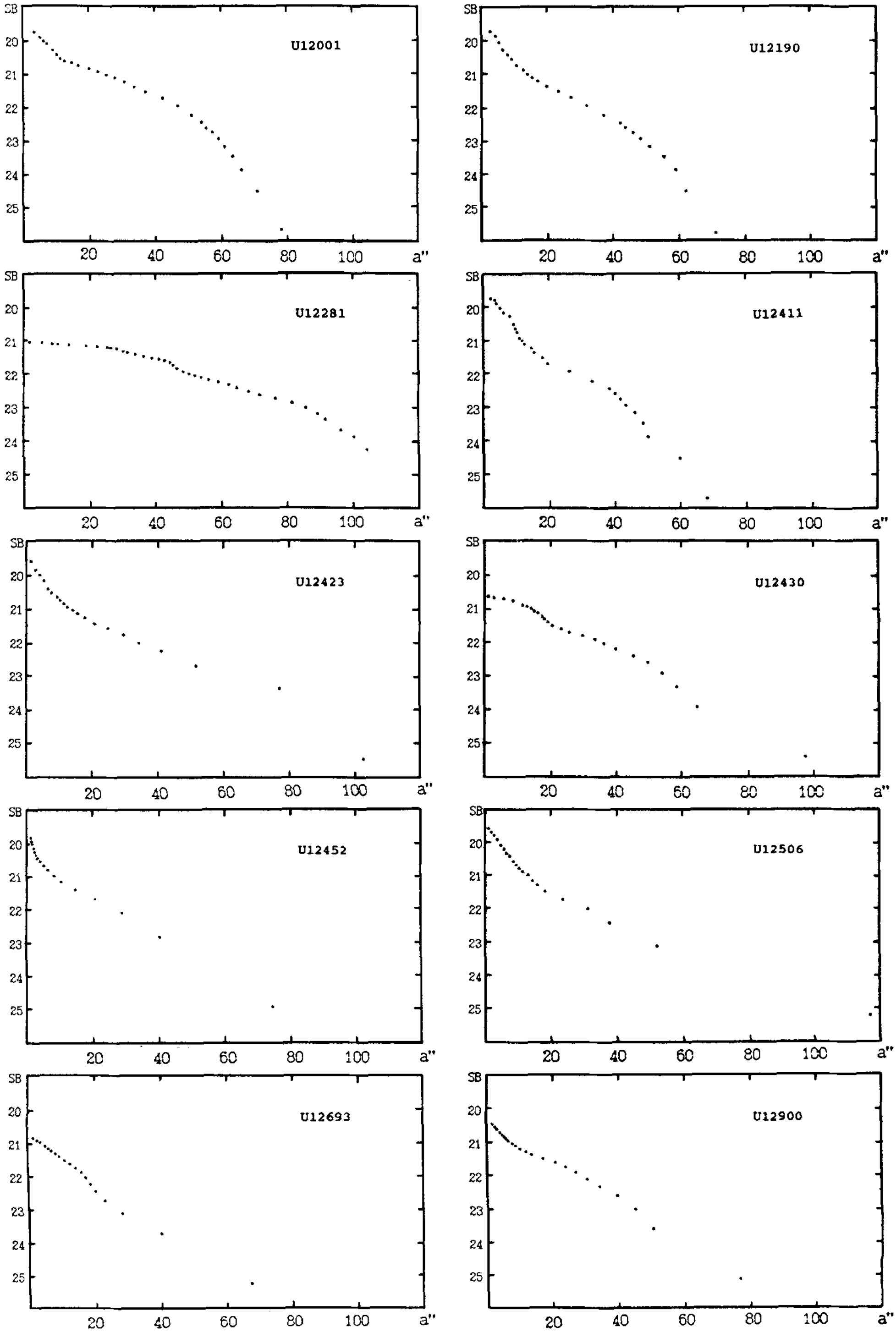

Figure 3 (*Continued*)

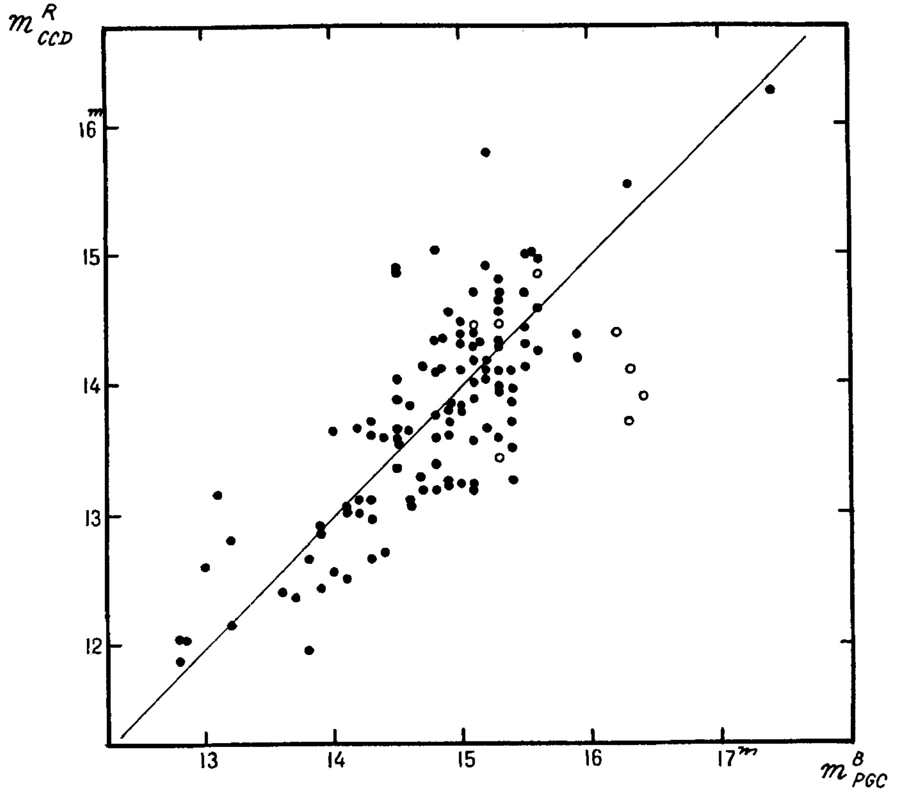

Figure 4 The red (CCD) magnitude versus the blue (PGC) one for flat galaxies.

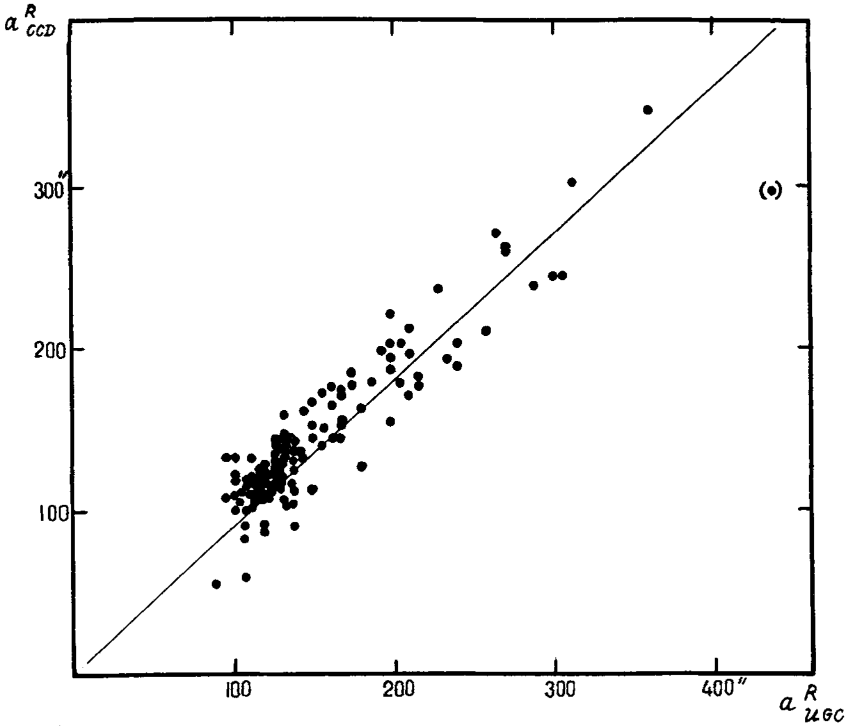

Figure 5 The red CCD angular diameter, measured at the level of 24 mag/arc second^2, versus the red UGC diameter for the flat galaxies.

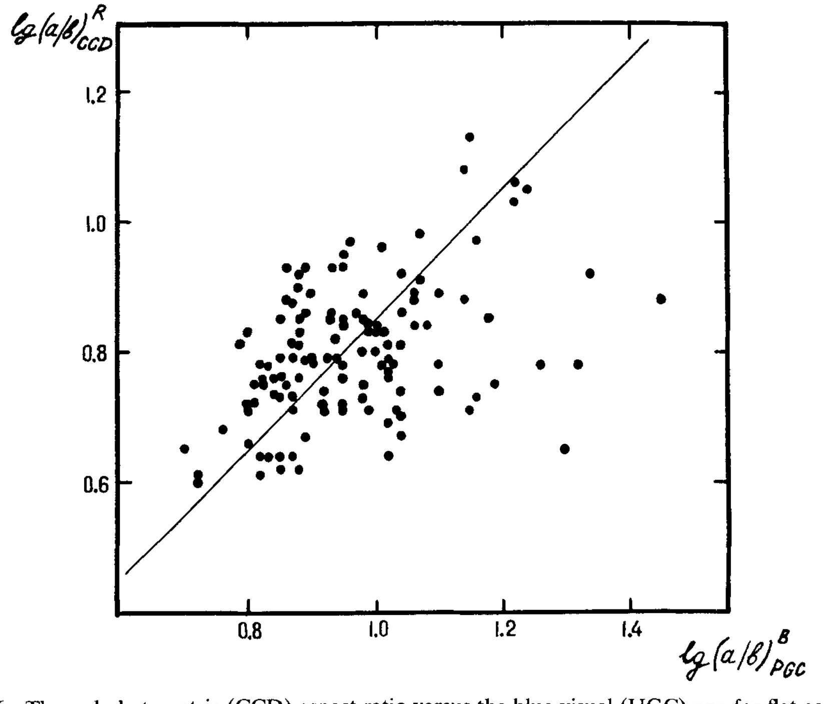

Figure 6 The red photometric (CCD) aspect ratio versus the blue visual (UGC) one for flat galaxies.

Table 2

SB	$\sigma(SB)$	*SB*	$\sigma(SB)$
$19^{m}.0$–$19^{m}.5$	$0^{m}.06$	$22^{m}.5$–$23^{m}.0$	$0^{m}.13$
19.5–20.0	0.04	23.0–23.5	0.13
20.0–20.5	0.07	23.5–24.0	0.21
20.5–21.0	0.06	24.0–24.5	0.30
21.0–21.5	0.07	24.5–25.0	0.33
21.5–22.0	0.08	>25.0	0.85
22.0–22.5	0.11		

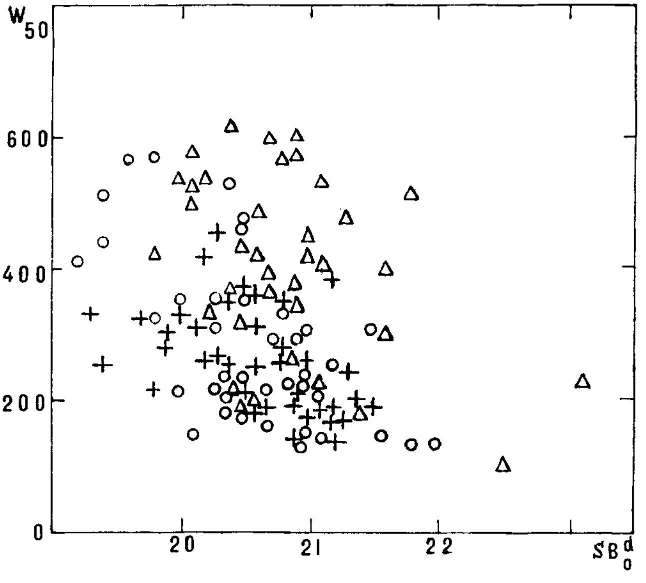

Figure 7 The 21 cm linewidth (in km/s) versus the surface brightness at the disk center (in mag/arc second^2) for the flat galaxies having different shapes of the luminosity profile. Open circles: the exponential profiles; triangles: objects with an apparent bulge (PI < 0); crosses: galaxies with PI > 0.

References

Borisenko, A. N., Vitkovskij, V. V., Zhelenkova, O. P., Kopylov, A. I., Markelov, S. V., Ryadchenko, V. P. and Shergin, V. S. 1990. *Astrofiz. Issled.* (*Izv. SAO*) **32,** 157.

Bottinelli, L., Gouguenheim, L., Fouque, P. and Paturel, G. 1990. *Astron. Astrophys. Suppl.* **82,** 391.

Cousins, A. W. 1976. *Mem. R.A.S.* **81,** 25.

Devies, J. I. 1990. *Mon. Not. R. Astron. Soc.* **245,** 350.

Freudling, W. 1990. *A search for streaming motion around the Hercules void,* Ph.D. Thesis, Cornell University.

Fouque, P. and Paturel, G. 1983. *Astron. Astrophys. Suppl.* **53,** 351.

Georgiev, Tz. B. 1991. *Asrtofiz. Issled.* (*Izv. SAO*) **33,** 213.

Haynes, M. P. and Giovanelli, R. 1992. (private communication).

Huchtmeier, W. K. and Richter, O. G. 1989. *A General Catalog of HI Observations of Galaxies* (Springer-Verlag, Berlin).

Karachentsev, I. 1989. *Astron. J.* **97,** 1566.

Karachentsev, I. 1991a. *Pis'ma Astron. Zh.* **17,** 485.

Karachentsev, I. 1991b. *Pis'ma Astron. Zh.* **17** (in press).

Karachentsev, I. and Zhou Xu 1991. *Pis'ma Astron. Zh.* **17,** 321.
Karachentsev, I., Karachentseva, V. and Parnovsky, S. 1993. *Flat Galaxies Catalogue,* in press. (FGC).
Meisels, A. 1985. *Astron. Astrophys.* **145,** 135.
Nilson, P. 1973. *Uppsala General Catalogue of Galaxies,* Uppsala Astron. Obs. Ann. **6**.
Nilson, P. 1974. *Catalogue of Selected non-UGC Galaxies,* Uppsala Astron. Obs. Report No. 5.
Paturel, G., Fouque, P., Bottinelli, L. and Gouguenheim, L. 1989. *Catalogue of Principal Galaxies* (Lyon) (PGC).
Richter, G. M. and Lorenz, H. 1989, private communication.
Skrutskie, M. F., Shure, M. A. and Beckwith, S. 1985. *Astrophys. J.* **299,** 303.
van der Kruit, P. C. and Searle, L. 1981. *Astron Astrophys.* **95,** 105.
van der Kruit, P. C. and Searle, L. 1982. *Astron Astrophys.* **110,** 61.
Valentijn, E. A. 1990. *Nature* **346,** 153.
Vaucouleurs, A. de and Longo, G. 1988. *Catalogue of visual and infrared photometry of galaxes* (University of Texas, Austin).
Watanabe, M. 1983. *Annals Tokyo Astron. Observ.* **19,** 121.
Zwicky, F., Herzog, E., Karpowicz, M., Kowal, C. T. and Wild, P. 1961–1968. *Catalogue of galaxies and of clusters of galaxies* (California Institute of Technology, Pasadena, vols. 1–6).